

Reviewer 1

This paper describes the development of a high space and time fossil fuel CO₂ inventory for Los Angeles. It is an important contribution to the literature. The paper covers the description of the data set well. The one thing I would recommend is that the authors take a broader view of the community they are trying to influence with their ideas. The introduction is very self-referential and pays little to no attention to CO₂ observing/modeling projects in Paris, Zurich, San Francisco, Boston and likely others. Helping the uninitiated reader to understand how this project relates to others should be a goal of the introduction and would make the paper more influential.

[[author]] greater context is achieved by adding text with references to a few of the cities other than those in which the author has been involved. These examples attempt to include those engaged in top-down/bottom-up convergent efforts. I could find no peer-reviewed information about CO₂ observing/modeling efforts in Zurich. The added text is:

“For example, ongoing efforts at integration of atmospheric measurements and bottom-up emissions information are taking place in Paris (Breon et al., 2015; Staufer et al., 2016), Boston (Sargent et al., 2018), Salt Lake City (Mitchell et al., 2018) and London (Font et al., 2015), to name a few.

17 **Reviewer 2**

18 General Comments

19 1. The Hestia data products provide bottom-up fossil fuel emissions at the urban scale with
20 building/street and hourly space-time resolution. The data feed into atmospheric CO₂ inversion
21 studies and can help guide to climate change mitigation options, includ- ing disaggregation of
22 national goals/policies to the local level. This paper focuses on the Los Angeles Megacity, the
23 Combined Statistical Area that includes Los Angeles, Orange, Riverside, San Bernardino, and
24 Ventura counties, providing CO₂ emissions results at a spatial resolution of 1km by 1km for the
25 years 2010-2015. The input data are from the Vulcan Project, adjusted where superior local and
26 downscaled data are available. It was found that the study area emitted 48.06 MtC/yr. Of note,
27 Hestia emissions were found to be 10.7% larger than the estimate by the local metropolitan
28 planning agency, the Southern California Association of Governments (SCAG).

29 2. The Hestia-LA data product, and the Vulcan dataset in general, are exciting advances in the
30 urban greenhouse gas emissions quantification field. In particular, the data product goes beyond
31 traditional carbon inventories used by city planning agencies to include a higher spatial and
32 temporal resolution. This makes the data product particularly exciting for the development of
33 highly impactful and targeted carbon reduction policies in cities.

34 Specific Comments

35 3. This reviewer has a keen interest in urban planning and policy-related efforts for greenhouse
36 gas emissions reduction in cities. As such, the comments are intended to help improve the
37 paper's accessibility to a planning/policy audience and help specify the policy-related
38 importance of the Hestia-LA work.

39 4. This work is of interest to a variety of readers, including policy makers and urban planning
40 professionals. With that in mind, I would recommend defining a few of the atmospheric-science-
41 specific words and phrases earlier on in the introduction, particularly "flux" and "inversion",
42 ideally in the context of other phrases that are more recognizable to the policy maker or
43 layperson (e.g., "emissions", "CO₂ emissions"). For example, the term "flux" begins to appear
44 regularly on page 3 (e.g., "flux measurements", "flux estimation", "surface fluxes"), and it could
45 be confusing to a reader who isn't used to the terminology. This would make the content more
46 accessible to policy audiences.

47 **[[author]] We have clarified the terms mentioned. On lines 86-87, we provide a definition of**
48 **"flux":**

49 **"....ground-based eddy flux (i.e. emissions of CO₂ into the atmosphere and/or CO₂ being removed from the**
50 **atmospheric by vegetation) measurements..."**

51 **On lines 132-134, we define the term "inversion":**

52 **"....atmospheric CO₂ inversion (i.e. an approach whereby CO₂ concentration measurements in the atmosphere are**
53 **combined with models of wind motions to infer what the emissions emanating from the surface must be)."**

54 **The importance of the policy application has been emphasized in the abstract by flipping the**
55 **order of the application to inversion and the application to policy.**

56 5. The introduction does a good job in describing the body of work on greenhouse gas
57 accounting in the urban environment, including the gap in existing methods that the Hestia
58 Project aims to address. The discussion of policy-related issues on p2-3 are good: lines 50-55

59 (contributions from city-based policies to meeting national/global commitments), 64-68 (data
60 and aggregation difficulties), 95-99 (translation to urban mitigation efforts). I would have liked
61 to see a few more lines on the benefits and drawbacks of policy-related/traditional greenhouse
62 gas emissions inventories (mentioned on p2, line 64 - note that these two citations do not actually
63 appear in the reference list). It would be good to reference the Global Protocol for Community-
64 scale GHG Emissions (GPC) here, as this is the current standard for city-based GHG inventories
65 in the policy world, used by both the C40 and GCoM (two organizations that are currently
66 mentioned in the paper). See <https://ghgprotocol.org/greenhouse-gas-protocol-accounting-reporting-standard-cities>. The paragraph on page 29, lines 672-683, does an excellent job of
67 describing the issues with traditional urban inventories and the benefit of the Hestia approach.
68 Could a few aspects of this description appear in the introduction?
69

70 [[author]] The missing references have been added to the reference section. The Fong et al.
71 reference is to the GPC. The introduction now has some of the conceptual material that the
72 reviewer notes, previously found later in the paper.

73 Text has been added on lines 82-87 that clarifies the potential benefit of the Hestia-style
74 approach:

75 “The need for greater granularity and specificity of emissions promises more efficient policy solutions. As all cities
76 reach beyond the existing “low hanging fruit” of emissions mitigation (i.e. those actions that are already planned for
77 other reasons, those that are simple and cost-plus), competition for limited resources and policy justification will
78 increase. Having information that can isolate the most efficient and effective emission reduction investments
79 (specific roadways/intersections, building subdivisions or commercial building clusters), will be at a premium.”

80 6. The data collection and processing effort involved in creating the Vulcan and Hestia datasets
81 are impressive and well-described. The types of emissions that are included and excluded from
82 the Vulcan dataset are detailed: the Vulcan dataset focuses on energy-related fossil fuel
83 emissions, thereby missing greenhouse gas emissions related to non-fossil fuel activities, such as
84 fugitive/evaporative emissions and direct industrial process emissions from activities such as
85 steel production (however, the text specifies that emissions from cement production are
86 included). It may be worth mentioning at this point that CH₄ and N₂O are not included (this is
87 mentioned on p24, but could be mentioned earlier – for example, on p6 the inclusion of carbon
88 monoxide is discussed, which could be a good place to put information about treatment of CH₄
89 and N₂O). Waste management is an important part of traditional city inventories, and the urban
90 planning/policy-making crowd may want to know if emissions from waste
91 decomposition/incineration are included/excluded from the dataset.

92 [[author]]: lines 141-142 now contains the following clarification:

93 “Emissions considered here are carbon dioxide only; other important greenhouse gases such as methane (CH₄) and
94 nitrous oxide (N₂O) are not included.”

95 Line 167 now contains the additional clarification:

96 “Similarly emissions associated with waste decay (organic or inorganic) are not included.”

97 7. The analysis of spatial clustering and local emissions “hotspots” is very interesting and could
98 potentially have direct policy/planning relevance. While not necessarily brand-new information
99 (high traffic flow and congestion are likely well known), the addition of the emissions
100 consequences could potentially open the door to new forms of carbon-related financing/policy
101 mechanisms.

102 8. Something that stands out in the abstract is the 10% difference in the model results and the
103 planning authority's GHG inventory. However, in the paragraphs on p24, a bit more information
104 is needed about the SCAG model to understand the comparison to Hestia and its relevance.
105 SCAG is described as "a regional greenhouse gas emissions inventory for a base year period of
106 1990-2009 with projections out to the year 2035." Are these both direct emissions inventories?
107 Does SCAG use a traditional accounting approach similar to the GPC or an approach closer to
108 Hestia's methodology? Is the purpose of comparison for validation of Hestia, or to demonstrate
109 the drawbacks in the SCAG inventory? A couple more lines about the SCAG methodology and
110 the purpose of the comparison will help clarify.

111 [[author]]: agreed. On line 584-585, we redraft the sentence to read:

112 "There are very few estimates that can serve as an assessment of the accuracy of the Hestia FFCO₂ emissions as few
113 inventory efforts have been accomplished at the sub-state spatial scale in the United States."

114 On lines 595-597, we add the sentence:

115 "We use only the reported scope 1 emissions which were based on the approach adopted by CARB based on
116 guidelines from the Intergovernmental Panel on Climate Change (CARB, 2010)."

117 9. In my opinion, the most important paragraph for policy makers is p30, lines 700- 713. Policy
118 makers/planner may be tempted to think, "We do these GHG inventories already, why should we
119 look at this tool?" That paragraph directly answers the question of why an urban planner/policy
120 maker should care about this work. I highly recommend bringing elements of this paragraph to
121 the introduction and/or abstract. Perhaps a few lines in the introduction that are specifically
122 directed at city planners and policy makers. I completely agree with the line, "The most
123 important attribute of the Hestia- LA approach, therefore, is the potential it offers for targeting
124 urban CO₂ reduction policy more efficiently." This hook deserves an earlier appearance in the
125 paper.

126 [[author]] some of the themes noted have been brought forward to lines 82-87. For example:

127 "The need for greater granularity and specificity of emissions promises more efficient policy solutions. As all cities
128 reach beyond the existing "low hanging fruit" of emissions mitigation (i.e. those actions that are already planned for
129 other reasons, those that are simple and cost-plus), competition for limited resources and policy justification will
130 increase. Having information that can isolate the most efficient and effective emission reduction investments
131 (specific roadways/intersections, building subdivisions or commercial building clusters), will be at a premium."

132 Technical Corrections

133 - As mentioned above, the two citations on p2, line 64, do not appear in the reference list - Typo
134 in y-axis label of Figure 10b.

135 [[author]]: Missing references have been added to the reference section. Figure 10b has been
136 corrected.

The Hestia Fossil Fuel CO₂ Emissions Data Product for the Los Angeles Megacity (Hestia-LA)

Kevin R. Gurney¹, Risa Patarasuk⁴, Jianming Liang^{2,3}, Yang Song², Darragh O’Keeffe⁵, Preeti Rao⁶, James R. Whetstone⁷, Riley M. Duren⁸, Annmarie Eldering⁸, Charles Miller⁸

¹School of Informatics, Computing, and Cyber Systems, Northern Arizona University, Flagstaff, AZ, USA

²School of Life Sciences, Arizona State University, Tempe AZ USA

³Now at ESRI, Redlands, CA USA

⁴Citrus County, Dept. of Systems Management, Lecanto, FL, USA

⁵Contra Costa County, Department of Information Technology, Martinez, CA, USA

⁶School for Environment and Sustainability, University of Michigan, Ann Arbor, MI, USA

⁷National Institute for Standards and Technology, Gaithersburg, MD, USA

⁸NASA Jet Propulsion Laboratory, California Institute of Technology, Pasadena, CA, USA

Correspondence to: Kevin R. Gurney (kevin.gurney@nau.edu)

Abstract. High-resolution bottom-up estimation provides a detailed guide to city greenhouse gas mitigation options, offering details that can increase the economic efficiency of emissions reduction options and synergize with other urban policy priorities at the human scale. As a critical constraint to urban atmospheric CO₂ inversion studies, bottom-up spatiotemporally-explicit emissions data products are also necessary to construct comprehensive urban CO₂ emission information systems useful for trend detection and emissions verification. The ‘Hestia Project’ is an effort to provide bottom-up granular fossil fuel (FFCO₂) emissions for the urban domain with building/street and hourly space-time resolution. Here, we report on the latest urban area for which a Hestia estimate has been completed – the Los Angeles Megacity, encompassing five counties: Los Angeles County, Orange County, Riverside County, San Bernardino County and Ventura County. We provide a complete description of the methods used to build the Hestia FFCO₂ emissions data product for the years 2010-2015. We find that the LA Basin emits 48.06 (± 5.3) MtC/yr, dominated by the onroad sector. Because of the uneven spatial distribution of emissions, 10% of the largest emitting gridcells account for 93.6%, 73.4%, 66.2%, and 45.3% of the industrial, commercial, onroad, and residential sector emissions, respectively. Hestia FFCO₂ emissions are 10.7% larger than the inventory estimate generated by the local metropolitan planning agency, a difference that is driven by the industrial and electricity production sectors. The detail of the Hestia-LA FFCO₂ emissions data product offers the potential for highly targeted, efficient urban greenhouse gas emissions mitigation policy. The Hestia-LA v2.5 emissions data product can be downloaded from National Institute of Standards and Technology repository (<https://doi.org/10.18434/T4/1502503>).

1 Introduction

Driven by the growth of fossil fuel energy demand, the amount of carbon dioxide (CO₂), the most important anthropogenic greenhouse gas (GHG) in the Earth’s atmosphere, recently reached an annual average global mean concentration of 402.8 ± 0.1 parts per million (ppm) on its way to doubling pre-industrial levels (IPCC, 2013; LeQuere et al., 2018). We have also witnessed the first time that the majority of world’s inhabitants reside in urban

Deleted: As a critical constraint to atmospheric CO₂ inversion studies, bottom-up spatiotemporally-explicit emissions data products are necessary to construct comprehensive CO₂ emission information systems useful for trend detection and emissions verification.

Deleted: is also useful as

Deleted: mitigation

Deleted: efficiency

Deleted: goals at the national to sub-urban spatial scale

Deleted: at the urban scale

Deleted: which is presented on a 1 km x 1 km grid

Deleted: the data repository at the

Deleted: combustion

185 areas. This trend, like atmospheric CO₂ levels, is intensifying. Projections show cities worldwide could add 2 to 3
 186 billion people this century and are projected to triple in area by 2030 (UN DESA 1015; Seto et al., 2012).

187 These two thresholds are linked—almost three-quarters of energy-related, atmospheric CO₂ emissions are driven by
 188 urban activity (Seto et al., 2014). If the world's top 50 emitting cities were counted as one country, that nation would
 189 rank third in emissions behind China and the United States (World Bank 2010). Indeed, urbanization is a factor
 190 shaping national contributions to internationally agreed emission reductions, as subnational governments are playing
 191 an increasing role in climate mitigation and adaptation policy implementation (Bulkeley 2010; Hsu et al., 2017).
 192 Furthermore, the pace of urbanization continues to increase and opportunities to avoid carbon “lock-in” - where
 193 relationships between technology, infrastructure, and urban form dictate decades of high-CO₂ development - are
 194 diminishing (Ürge-Vorsatz et al., 2018; Seto et al., 2016; Erickson et al., 2015).

195 Motivated by these numerical realities and the recognition that low-emission development is consistent with a
 196 variety of other co-benefits (e.g. air quality improvement), cities are taking steps to mitigate their CO₂ emissions
 197 (Rosenzweig et al., 2010; Hsu et al., 2015; Watts 2017). For example, 9120 cities representing over 770 million
 198 people (10.5% of global population) have committed to the Global Covenant of Mayors (GCoM) to promote and
 199 support action to combat climate change (GCoM, 2018). Over 90 large cities, as part of the C40 network, have
 200 similarly committed to mitigation actions with demonstrable progress. However, the scale of actual reductions
 201 remains modest, despite the many pledges and initial progress. For example, a recent study reviewed 228 cities
 202 pledged to reduce 454 megatons of CO₂ per year by 2020 (Erickson and Lazarus, 2012). Were they to meet these
 203 commitments, the reduction would account for about 3% of current global urban emissions and less than 1% of total
 204 global emissions projected for 2020. More important, there is a need for timely information to manage and assess
 205 the performance of implemented mitigation efforts and policies (Bellassen et al., 2015).

206 One of the barriers to targeting a deeper list of emission reduction activities is the limited amount of actionable
 207 emissions information at scales where human activity occurs: individual buildings, vehicles, parks, factories and
 208 power plants (Gurney et al., 2015). These are the scales at which interventions in CO₂-emitting activity must occur.
 209 Hence, the emissions magnitude and driving forces of those emissions must be understood and quantified at the
 210 “human” scale to make efficient (i.e. prioritizing the largest available emitting activities/locales) mitigation choices
 211 and to capture the urban co-benefits that also occur at this scale (e.g. improve traffic congestion, walkability, green
 212 space). Similarly, a key obstacle to assessing progress is a lack of independent atmospheric evaluation (ideally
 213 consistent in space and time with the human-scale emissions mapping) (Duren and Miller, 2011).

214 Existing methods and tools to account for urban emissions have been developed primarily in the non-profit
 215 community (WRI/WBCSD, 2004; Fong et al., 2014). In spite of these important efforts, most cities lack
 216 independent, comprehensive and comparable sources of data and information to drive and/or adjust these
 217 frameworks. Furthermore, the existing tools and methods are designed at an aggregate level (i.e. whole city, whole
 218 province), missing the most important scale—sub-city—and hence provide limited actionable information. The need
 219 for greater granularity and specificity of emissions promises more efficient policy solutions. As all cities reach
 220 beyond the existing “low hanging fruit” of emissions mitigation (i.e. those actions that are already planned for other

221 reasons, those that are simple and cost-plus), competition for limited resources and policy justification will increase.
222 Having information that can isolate the most efficient and effective emission reduction investments (specific
223 roadways/intersections, building subdivisions or commercial building clusters) will be at a premium.

224 The scientific community has begun to build information systems aimed at providing independent assessment of
225 urban CO₂ emissions. Through a combination of atmospheric measurements, atmospheric transport modeling and
226 data-driven “bottom-up” estimation, the scientific community is exploring different methodologies, applications,
227 and uncertainty estimation of these approaches (Hutyra et al., 2014). Atmospheric monitoring includes ground-based
228 CO₂ concentration measurements (McKain et al., 2012; Djuricin et al., 2010; Miles et al., 2017; Turnbull et al.,
229 2015; Verhulst et al., 2017), ground-based eddy flux (i.e. emissions of CO₂ into the atmosphere and/or CO₂ being
230 removed from the atmospheric by vegetation) measurements (Christen 2014; Crawford and Christen 2014;
231 Grimmond et al., 2002; Menzer et al., 2015; Velasco and Roth 2010; Velasco et al., 2005), aircraft-based flux
232 measurements (Mays et al., 2009; Cambaliza et al., 2014; 2015) and whole-column abundances from both ground,
233 and space-based, remote sensing platforms (Wunch et al., 2009; Kort et al., 2012; Wong et al., 2015; Schwandner et
234 al., 2018).

235 “Bottom-up” approaches, by contrast, include a mixture of direct flux measurement, indirect measurement and
236 modeling. Common among the bottom-up approaches are those that include flux estimation based on a combination
237 of activity data (population, number of vehicles, building floor area) and emission factors (amount of CO₂ emitted
238 per activity), socioeconomic regression modeling, or scaling from aggregate fuel consumption (VandeWeghe and
239 Kennedy, 2007; Shu and Lam, 2011; Zhou and Gurney, 2011; Gurney et al., 2012; Jones and Kammen, 2014;
240 Ramaswami and Chavez, 2013; Patarasuk et al., 2016; Porse et al., 2016). Direct end-of-pipe flux monitoring is
241 often used for large point sources such as power plants (Gurney et al., 2016). Indirect fluxes (those occurring outside
242 of the domain of interest but driven by activity within) can be estimated through either direct atmospheric
243 measurement (and apportioned to the domain of interest) or can be modeled through process-based (Clark and
244 Chester 2017) or economic input-output models (Ramaswami et al., 2008).

245 Integration of bottom-up urban flux estimation with atmospheric monitoring has been achieved with atmospheric
246 inverse modeling, an approach whereby surface fluxes are estimated from a best fit between bottom-up estimation
247 and fluxes inferred, via atmospheric transport modeling, from atmospheric concentrations (Lauvaux et al., 2013;
248 Lauvaux et al., 2016; Breon et al., 2015; Davis et al., 2017). Though the various measurement and modeling
249 components continue to be tested, integration offers an urban anthropogenic CO₂ information system which can
250 provide accuracy, emissions process information, and spatiotemporal detail. This combination of attributes satisfies
251 a number of urgent requirements. For example, it can offer the means to evaluate urban emissions mitigation efforts
252 by assessing urban trends. Space, time, and process detail of emitting activity can guide mitigation efforts,
253 illuminating where efficient opportunities exist to maximize reductions or focus new efforts. Finally, emissions
254 quantification is also seen as a potentially powerful metric with which to better understand the urbanization process
255 itself, given the importance of energy consumption to the evolution of cities.

The Hestia Project was begun to estimate bottom-up urban fossil fuel CO₂ (FFCO₂) fluxes for use within integrated flux information systems. Begun in the city of Indianapolis, the Hestia effort is now part of a larger experiment that includes many of the modeling and measurement aspects described above. Referred to as the Indianapolis Flux Experiment (INFLUX), this integrated effort has emerged to test and explore quantification and uncertainties of the urban CO₂ and methane (CH₄) measurement and modeling approaches using Indianapolis as the testbed experimental environment (Whetstone et al., 2018; Davis et al., 2017).

Because urban areas differ in key attributes such as size, geography, and emission sector composition, multiple cities are now being used to test aspects of anthropogenic CO₂ monitoring and modeling. For example, ongoing efforts at integration of atmospheric measurements and bottom-up emissions information are taking place in Paris (Breon et al., 2015; Staufer et al., 2016), Boston (Sargent et al., 2018), Salt Lake City (Mitchell et al., 2018) and London (Font et al., 2015), to name a few. The Hestia approach has been used in a number of these urban domains. Here, we provide the methods and results from one of those urban domains, the Los Angeles Basin Megacity. The Hestia-LA effort was developed under the Megacities Carbon framework (<https://megacities.jpl.nasa.gov/portal/>). It was designed to serve the Megacities Carbon Project in a similar capacity to its role in INFLUX. The Hestia-LA result is unique in that it is the first high-resolution spatiotemporally-explicit inventory of FFCO₂ emissions centered over a megacity. A preliminary version of Hestia-LA containing only the transportation sector emissions was reported by Rao et al. (2017). While emphasis thus far has been focused on atmospheric CH₄ monitoring analyses in the LA megacity (Carranza et al., 2017; Wong et al., 2016; Verhulst et al., 2017; Hopkins et al., 2016), work is ongoing to use the extensive atmospheric CO₂ observing capacity in the Los Angeles domain (e.g. Newman et al., 2016; Feng et al., 2016; Wong et al., 2015; Wunch et al., 2009) within an atmospheric CO₂ inversion (i.e. an approach whereby CO₂ concentration measurements in the atmosphere are combined with models of wind motions to infer what the emissions emanating from the surface must be).

In this paper, we describe the study domain, the input data, uncertainty, and the methods used to generate the Hestia-LA (v2.5) data product and provide descriptive statistics at various scales of aggregation. We compare the Hestia results to the metro region planning authority estimate and place the results in the context of urban greenhouse gas mitigation. We discuss known gaps and weaknesses in the approach and goals for future work.

2 Methods

2.1 Study Domain

The Los Angeles metropolitan area is the second-largest metropolitan area in the United States and one of the largest metropolitan areas in the world. Under the definition of the Metropolitan Statistical Area (MSA) by the U.S. Office of Management and Budget, Metropolitan Los Angeles consists of Los Angeles and Orange counties with a land area of 12,562 km² and a population of 9,819,000. The Greater Los Angeles Area, as a Combined Statistical Area (CSA) defined by the U.S. Census Bureau, encompasses the three additional counties of Ventura, Riverside, and San Bernardino with a total land area of 87,945 km² and an estimated population of 18,550,288 in 2014. The Hestia-LA FFCO₂ emissions data product covers the complete geographic extent of these five counties including the Eastern,

relatively non-urbanized portions of San Bernardino and Riverside counties. Airport emissions associated with aircraft up to 3000 feet are included as are marine shipping emissions out to 12 nautical miles from the coastal boundary. Emissions considered here are carbon dioxide only; other important greenhouse gases such as methane (CH₄) and nitrous oxide (N₂O) are not included.



Figure 1: The Hestia-LA urban domain

2.2 Input data

Input data to the Hestia-LA data product are supplied by output of the Vulcan Project (Figure 2), a quantification of FFCO₂ emissions at fine space and time scales for the entire US landscape (Gurney et al., 2009) The Hestia-LA process extracts these results for the five counties within the Hestia-LA domain and adjusts these estimates where superior local data are available and further downscales/distributes the Vulcan v3.0 results to buildings and street segments. Details of the Vulcan v3.0 methodology is provided elsewhere (Gurney et al., 2018). Here, we summarize the Vulcan v3.0 methods and then provide greater detail regarding the Hestia-LA processing of that data to high-resolution space/time scales.

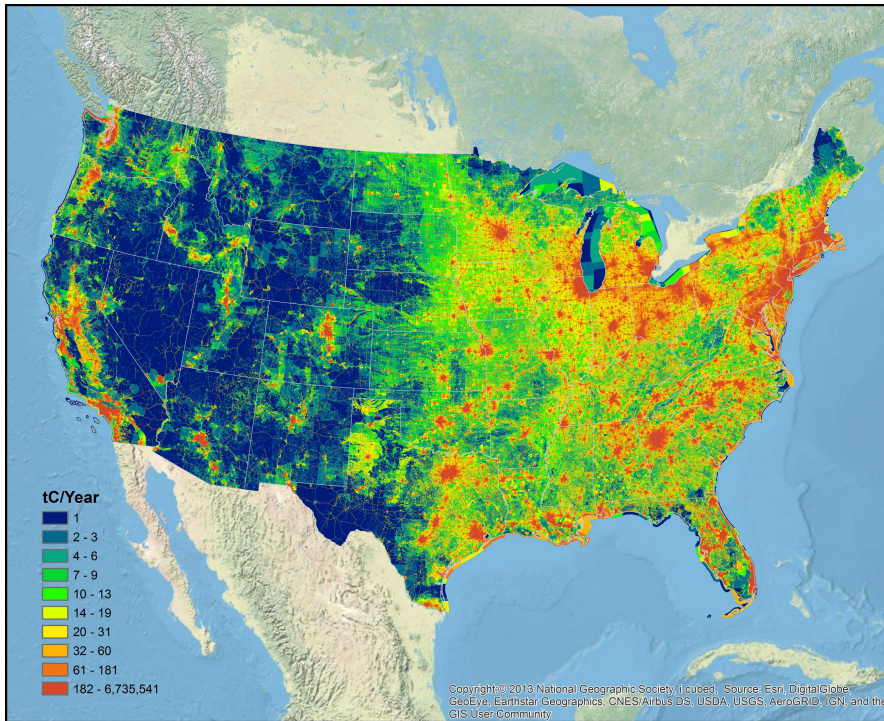


Figure 2: Total annual FFCO₂ emissions for the year 2011 from the Vulcan v3.0 output.

The Vulcan v3.0 input data (the output of which is the input for the Hestia-LA) are organized following nine economic sector divisions (see Table 1) - residential, commercial, industrial, electricity production, onroad, nonroad, railroad, commercial marine vessel, and airport. Also included are emissions associated with the calcining process in the production of cement. The data sources within each sector are either acquired as FFCO₂ emissions (the onroad sector and most of the nonroad and electricity production sectors) or as carbon monoxide (CO) emissions (all other sectors) and transformed to FFCO₂ emissions via emission factors. Furthermore, the data sources are represented geographically as either geocoded emitting locations (“point”) or as spatial aggregates (“nonpoint” or area-based emissions). Point sources are stationary emitting entities identified to a geocoded location such as industrial facilities in which emissions exit through a stack or identifiable exhaust feature (USEPA, 2015a). Area or nonpoint source emissions are not inventoried at the facility-level but represent diffuse emissions within an individual U.S. county. Because the focus of the current study is CO₂ emissions resulting from the combustion of a fossil fuels, fugitive or evaporative emissions are not included nor are “process” emissions, for example, associated with high-temperature metallurgical processes. Similarly emissions associated with waste decay (organic or inorganic) are not included.

Much of the input data for Vulcan v3.0 are acquired from the Environmental Protection Agency's (EPA) National Emission Inventory (NEI) for the year 2011 (referred to hereafter as the "2011 NEI") which is a comprehensive inventory of all criteria air pollutants (CAPs) and hazardous air pollutants (HAPs) across the United States (USEPA, 2015b). All of the individual record-level reporting in the 2011 NEI comes with a source classification code (SCC) which codifies the general emission technology, fuel type used, and sector (USEPA 1995).

FFCO₂ emissions from the electricity production sector are primarily retrieved from two sources other than the 2011 NEI. The first is the EPA's Clean Air Markets Division (CAMD) data (USEPA, 2015c) which reports FFCO₂ emissions at geocoded electricity production facility locations. The second is the Department of Energy's Energy Information Administration (DOE EIA) reporting data (DOE/EIA, 2003) which reports fuel consumption at geocoded electricity production facility locations. Some electricity production emissions are retrieved from the 2011 NEI (as CO emissions). Overlap between these three data sources is eliminated via preference in the order listed above. A detailed comparison made between the CAMD and EIA FFCO₂ emissions along with greater detail regarding data sources, data processing and procedures can be found in Quick et al., (2014) and Gurney et al. (2014; 2016; 2018).

The 2011 onroad FFCO₂ emissions are retrieved from the Emissions FACtors 2014 model (EMFAC2014), produced by the California Air Resources Board (CARB, 2014). Onroad transportation represents all mobile transport using paved roadways and include both private and commercial vehicles of many individual classes (e.g., passenger vehicles, buses, light duty trucks, etc). The nonroad sector, by contrast, includes all surface mobile vehicles that do not travel on designated paved roads surface and include a large class of vehicles such as construction equipment (e.g., bulldozers, backhoes, etc.), ATVs, snowmobiles, and airport fueling vehicles. The nonroad emissions are derived from the 2011 NEI reporting of nonroad CO emissions. Airport emissions include all the emissions emanating from aircraft during their taxi, takeoff, landing cycles up to 3000 feet and are derived from the 2011 NEI point reporting. Other activities occurring at airports resulting in FFCO₂ emissions are captured in the commercial building sector (building heating) or the nonroad sector (baggage vehicles), sourced to the 2011 NEI nonpoint, 2011 NEI point and 2011 NEI nonroad reporting. Railroad emissions include passenger and freight rail travel and are sourced to the 2011 NEI nonpoint and point reporting. Commercial marine vessels (CMV) include all commercial-based aquatic vessels on either ocean or freshwater sourced to the 2011 NEI nonpoint reporting. Personal aquatic vehicles such as pleasure craft and sailboats are included in the nonroad sector. Emissions associated with cement calcining are included given its potential size and the tradition of including it with CO₂ inventories and use information from multiple sources (PCA, 2006; USGS, 2003; IPCC, 2006).

The FFCO₂ emissions input to the Hestia system from the Vulcan v3.0 output is associated with spatial elements represented by points, lines and polygons, depending upon the data source, the sector and the available spatial proxy data (Table 1). Further spatialization and temporalization occurs in the Hestia system.

Table 1. Data sources used in the spatiotemporal distribution of FFCO₂ emissions (text provides acronym explanations and sources).

| Sector/type | Emissions Data Source | Original spatial resolution/information | Spatial distribution | Temporal distribution |
|-------------|-----------------------|---|----------------------|-----------------------|
|-------------|-----------------------|---|----------------------|-----------------------|

| | | | | |
|--------------------------------|---|---|--|--------------------------------------|
| Onroad | EMFAC ^a , EPA NEI ^b onroad | County, road class, vehicle class | SCAG AADT ^c | PeMS ^d , CCS ^e |
| Electricity production | CAMD ^f CO ₂ , EIA ^g fuel, EPA NEI point CO | Lat/lon, fuel type, technology | EPA NEI Lat/Lon, Google Earth | CAMD, EIA and EPA |
| Residential nonpoint buildings | EPA NEI nonpoint CO | County, fuel type | SCAG Parcel, floor area, DOE RECS NE-EUI ^h , LA County building footprint | eQUEST ⁱ |
| Nonroad | NEI nonpoint CO | County, vehicle class | EPA spatial surrogates (vehicle class specific) | EPA temporal surrogates (by SCC) |
| Airport | EPA NEI point CO | Lat/lon, aircraft class | Lat/Lon | LAWA ^k |
| Commercial nonpoint buildings | EPA NEI nonpoint CO | County, fuel | SCAG Parcel, floor area, DOE CBECS NE-EUI ^l | eQUEST |
| Commercial point sources | EPA NEI point CO | Lat/lon, fuel type, combustion technology | EPA NEI Lat/Lon, Google Earth | eQUEST |
| Industrial point sources | EPA NEI point CO | Lat/Lon, fuel type, combustion technology | EPA NEI Lat/Lon, Google Earth | EPA temporal surrogates (by SCC) |
| Industrial nonpoint buildings | EPA NEI nonpoint CO | County, fuel type | SCAG-Parcel, floor area, DOE MECS NE-EUI ^m | eQUEST |
| Commercial Marine Vessels | EPA NEI nonpoint CO | County, fuel type, port/underway | MEM ⁿ | MEM |
| Railroad | EPA NEI nonpoint CO, EPA NEI point CO | County, fuel type, segment | EPA NEI rail shapefile and density distribution | EPA temporal surrogates (by SCC) |

- a. Emissions Factors Model
- b. Environmental Protection Agency, National Emissions Inventory
- c. Southern California Association of Governments, Annual Average Daily Traffic
- d. Performance Measurement System
- e. Continuous Count Stations
- f. Clean Air Markets Division
- g. Energy Information Administration
- h. Department of Energy Residential Energy Consumption Survey, non-electric energy use intensity
- i. Quick Energy Simulation Tool
- j. Source Classification Code
- k. Los Angeles World Airport
- l. Department of Energy Commercial Energy Consumption Survey, non-electric energy use intensity
- m. Department of Energy Manufacturing Energy Consumption Survey, non-electric energy use intensity
- n. Marine Emissions Model

To estimate FFCO₂ emissions as a multiyear time series from 2010 to 2015, the results for the year 2011 were scaled using sector/state/fuel consumption data (thermal units) from the DOE EIA (DOE/EIA, 2018). The electricity production sector was an exception to this approach where year-specific data was available in the CAMD and EIA data sources. Ratios were constructed relative to the year 2011 in all SEDS sector designations for each US state. The ratio values are applied to the annual totals in each of the sector/fuel categories specific to the state FIPS code.

2.3 Space/time processing

2.3.1 Residential, commercial, industrial nonpoint buildings

The general approach to spatializing the residential, commercial and industrial nonpoint FFCO₂ emissions is to allocate the county-scale, fuel-specific annual sector totals to individual buildings (or parcels) using data on building type, building age, total floor area, energy use intensity, and location.

A portion of the Hestia-LA building information were provided by the Southern California Association of Governments (SCAG) (SCAG, 2012) and included building type, age, floor area, and location. The spatial resolution of this information was at the land parcel scale (larger than the building footprint). Building footprint data was available in the county of Los Angeles only which offered additional building floor area information needed to correct some floor area values in the SCAG parcel data (LAC, 2016). For example, a large number of commercial

parcels with zero floor area were found in the Riverside County data which were visually inspected in Google Earth to contain qualifying buildings. These floor area values were corrected through the combination of the Census block-group General Building Stock (GBS) database from the Federal Emergency Management Agency (FEMA) (FEMA, 2017) and the National Land Cover Database 2011 (NLCD) which classifies the US land surface in 30m pixels (Homer et al., 2015).

Building energy use intensity was derived from data gathered by the DOE EIA and the California Energy Commission (CEC). The DOE EIA Commercial Buildings Energy Consumption Survey (CBECS), Manufacturing Energy Consumption Survey (MECS), and Residential Energy Consumption Survey (RECS) represent regional surveys of building energy consumption categorized by building type, fuel type, and age cohort (RECS, 2013; CBECS, 2016; MECS, 2010). Data for the Pacific West Census Division was used and in the case of the commercial sector, was appended by the CECs Commercial End-Use Survey (CEUS) data (CEC, 2006).

In the residential sector the non-electric energy use intensity (NE-EUI) was calculated from the reported energy consumed and total floor area sampled specific to five building types (Table 2) in the 2009 RECS survey. This was additionally categorized by fuel type (natural gas and fuel oil) and two age cohorts (pre-1980, post-1979).

Table 2. Residential NE-EUI survey values by building type from the Residential Energy Consumption Survey (RECS)

| RECS building type | Pre-1980 NG NE-EUI (kbtu/ft ²) | Post-1979 NG NE-EUI (kbtu/ft ²) | Pre-1980 Fuel oil NE-EUI (kbtu/ft ²) | Post-1979 Fuel oil NE-EUI (kbtu/ft ²) |
|---|--|---|--|---|
| Mobile home | 52.56 | 22.90 | NA* | NA |
| Single-family detached house | 24.53 | 18.00 | 18.87 | 7.23 |
| Single-family attached house | 42.56 | 32.38 | NA | NA |
| Apartment building with 2-4 units | 27.84 | 42.27 | NA | NA |
| Apartment building with 5 or more units | 17.21 | 30.85 | NA | NA |

* "NA" – not applicable. This indicates that there was no fuel consumption of this type evident from the survey data.

In the commercial sector, the NE-EUI was similarly calculated from the 2012 CBECS energy consumption microdata and total floor area sampled specific to twenty building types, two fuel types (natural gas and fuel oil) and two age cohorts (pre-1980 and post-1979). However, the sampling for the two age cohorts was insufficient to generate estimates and the age distinction was eliminated. Furthermore, where the sample sizes remained small, NE-EUI data from the CEUS was used in place of CBECS estimates (7 of 20 building types qualified). As the CEUS follows a building typology different from CBECS, a crosswalk of building types between the two datasets was necessary (Table 3).

Table 3. Building type crosswalk and NE-EUI values for commercial buildings derived from the CBECS and CUES databases

| CBECS building class | CUES building class | NG NE-EUI (kbtu/ft ²) | Fuel oil NE-EUI (kbtu/ft ²) |
|---------------------------|--------------------------|-----------------------------------|---|
| Vacant | Miscellaneous | 9.3 | 2.5 |
| Office | All Offices | 17.9* | 1.67 |
| Laboratory | Miscellaneous | 174.7 | 0.93 |
| Nonrefrigerated warehouse | Unrefrigerated Warehouse | 3.1* | 1.03 |
| Food sales | Food Store | 27.6* | 2.5 |
| Public order and safety | Miscellaneous | 58.2 | 2.09 |
| Outpatient health care | Health | 29.1 | 3.05 |

| | | | |
|------------------------|------------------------|-------|-------|
| Refrigerated warehouse | Refrigerated Warehouse | 5.6* | 2.5 |
| Religious worship | Miscellaneous | 35.7 | 0.00 |
| Public assembly | Miscellaneous | 26.5 | 0.23 |
| Education | College, School | 25.1* | 1.7 |
| Food service | Restaurant | 210* | 100.5 |
| Inpatient health care | Health | 113.9 | 2.6 |
| Nursing | Health | 67.4 | 1.2 |
| Lodging | Lodging | 42.4* | 1.4 |
| Strip shopping mall | Retail | 62.7 | 2.5 |
| Enclosed mall | Retail | 4.8 | 0.02 |
| Retail other than mall | Retail | 13.6 | 16.7 |
| Service | Miscellaneous | 34.2 | 0.45 |
| Other | Miscellaneous | 18.5 | 5.3 |

* NE-EUI uses the CUES NE-EUI value due to sampling limitations in the CBECS data.

Unlike the commercial and residential survey data, the 2010 MECS survey data does not quantify energy consumption for individually sampled buildings but rather reports the sum of the sampled buildings within each census region categorized by manufacturing sector. The resulting NE-EUI values are shown in in Table 4. Like the commercial data, there was inadequate sampling to justify two age cohorts.

Table 4. Industrial NE-EUI survey values from the DOE EIA MECS database

| MECS Class | NG NE-EUI (kbtu/ft²) | Fuel oil NE-EUI (kbtu/ft²) |
|---|-------------------------|-------------------------------|
| Food | 519.3 | 30.5 |
| Beverage and Tobacco Products | 162.4 | 8.5 |
| Textile Mills | 144.9 | 9.3 |
| Textile Product Mills | 63.4 | 0 |
| Apparel | 35.1 | 0 |
| Leather and Allied Products | 66.7 | 0 |
| Wood Products | 76.6 | 49.5 |
| Paper | 672.8 | 69.1 |
| Printing and Related Support | 96.6 | 0 |
| Petroleum and Coal Products | 9766.0 | 436.2 |
| Chemicals | 2126.3 | 17.9 |
| Plastics and Rubber Products | 124.7 | 2.4 |
| Nonmetallic Mineral Products | 556.0 | 48.9 |
| Primary Metals | 895.0 | 16.7 |
| Fabricated Metal Products | 124.2 | 2.3 |
| Machinery | 78.6 | 3.3 |
| Computer and Electronic Products | 80.0 | 0 |
| Electrical Equip., Appliances, and Components | 133.3 | 3.7 |
| Transportation Equipment | 100.6 | 4.0 |
| Furniture and Related Products | 28.6 | 0 |
| Miscellaneous | 44.7 | 2.8 |

The NE-EUI values derived from the CBECS/RECS/MECS and CEUS survey data reflect the total building fuel consumption for a specific fuel in a census region divided by the total floor area of all buildings in that census region consuming that fuel. This generates a mean building NE-EUI value. Actual buildings will vary around that mean value for a variety of reasons including different occupancy schedules, different energy efficiencies (in the envelope or heating/cooling system), different microclimate, and other physical/behavioral characteristics. Furthermore, the NE-EUI value applied in this way will not capture the reality that some buildings do not use fossil fuel (electricity-only buildings) or that some buildings use one fossil fuel only versus another or use a mix of fuels in a proportion

different from the county total. Hence, each building will be allocated a mix of fossil fuel consumption identical to the county total.

2.3.1.1 Spatial distribution

The county-scale commercial, residential and industrial nonpoint FFCO₂ emissions are allocated to each land parcel in proportion to the product of the NE-EUI and the total floor area,

$$EC(b)_s^f = NE_EUI_s^f FA(b) \quad (1)$$

where the energy consumed, EC , in each building, b , is the product of the NE-EUI value, NE_EUI , and the floor area, FA , for each fuel, f , and each building in sector, s . The total energy consumed, TEC , within the county for a sector, s , is the sum of all the EC values across the N buildings in the sector,

$$TEC_s^f = \sum_{b=1}^N EC(b)_s^f \quad (2)$$

To convert this to FFCO₂ emissions, we first calculate the fraction of the total energy consumption associated with each building,

$$F(b)_s^f = \frac{EC(b)_s^f}{TEC_s^f} \quad (3)$$

where, F is the fraction of TEC consumed in building, b , of sector s . This is then used to distribute the county total FFCO₂ emissions as,

$$E(b)_s^f = E_s^f F(b)_s^f \quad (4)$$

where E_s is the FFCO₂ emissions either for the county or for building, b , and fuel. In allocating emissions from coal consumptions, however, NE_EUI takes the value of “1” for all building types so that the allocated emission in a building is directly proportional to the floor area.

2.3.1.2 Temporal distribution

The hourly time structure for buildings in the residential and commercial sectors are created via the use of eQUEST, a building energy simulation tool run for each of the building classes listed in Table 2 and Table 3 and using only the temporal structure of the energy consumption output (Hirsch & Associates, 2004). The model domain is specified as the city of Los Angeles for the year 2011 with TMY weather data from the DOE (Marion and Urban, 1995). The mean building area is provided by the parcel data as described previously.

For the industrial buildings, a temporal profile representing the mean of industrial point source temporal surrogates provided by EPA, are used (USEPA, 2015a). Figure 3 shows the hourly time profile during a one-week period in April for a selected building in the residential and commercial sector, respectively.

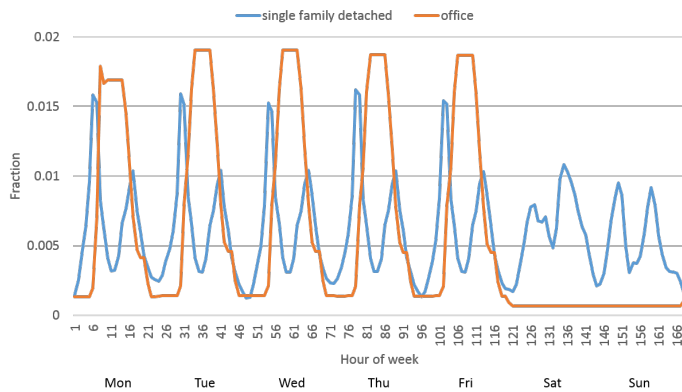


Figure 3. Energy consumption intensity (hourly fraction) from an eQUEST simulation on the average week in 2011 for two types of buildings: “single family detached house” and “office”.

2.3.2 Industrial and commercial point sources

Little space/time processing is required for industrial and commercial point source emissions since they are geocoded to specific facilities/emitting stacks or similar identifiable emission points. However, visual inspection of the point source locations in GIS suggested potential geocoding errors. Point source locations were reviewed by searching facility names to an online address search or via the EPA’s Facility Registry Service (FRS) which can link the facility in question to all the reporting made to the federal government under other environmental regulations (USEPA, 2013). This often returns a more accurate physical location. The geolocations considered inaccurate were manually corrected. Out of the total 192 facilities with corrected locations, 13 were moved a distance of between 924 and 1022 km while the remaining 179 were moved 0.5 km or less. The large magnitude location changes were likely transcription errors when originally recording the location coordinates.

A given commercial or industrial point source is typically composed of multiple emission processes or units. For example, in Los Angeles County, the 2011 NEI reports a total of 3409 emission records at 842 individual facilities. In some cases, the multiple emitting points at a facility are not at exactly the same geocoded point but may represent different emitting points at a facility that occupies a large area of land. Most often, however, all emitting points at a given facility are geocoded to the same latitude and longitude.

The sub-annual temporal distribution for the commercial and industrial point source emissions used temporal surrogate profiles provided by the EPA, linked according to the SCC of the emission record (USEPA, 2015a).

2.3.3 Electricity production

As described in Section 2.2, three different data sources are used to quantify the FFCO₂ emissions in the Hestia-LA domain: the Clean Air Markets Division (CAMD), the DOE-EIA reporting and 2011 NEI CO emissions data. In 2011 there were a total of 34 CAMD facilities, 228 EIA facilities and 147 NEI facilities (reported through the NEI

2011 point source fileset) in the Hestia-LA domain. Total electricity production emissions in the domain was 6.21 MtC/year exclusive of biogenic fuels and 6.68 MtC/year with biogenics included. The CAMD data is reported at hourly resolution, while the DOE EIA data is reported at monthly resolution and the 2011 NEI data is reported at annual resolution only. Reduction of all data to an hourly time increment was achieved by maintaining constant emissions within a month or year for the DOE EIA and 2011 NEI data, respectively.

2.3.4 Onroad

A preliminary version of the Hestia-LA onroad emissions estimates were presented by Rao et al. (2017). The version presented here uses updated data and Hestia methodologies.

2.3.4.1 Temporal distribution

The Hestia-LA onroad FFCO₂ emissions input are retrieved from the Vulcan v3.0 output spatialized to specific road segments in the Hestia-LA domain and categorized by vehicle class/fuel. Hence, no further spatialization was required.

Construction of the temporal distribution in the Hestia system relies upon the California Department of Transportation (CalTrans) Performance Measurement System (PeMS) (PeMS, 2018). This dataset contains 2011 traffic count data collected at 5 min intervals at measuring stations along freeways and principal arterials and along some minor arterials and collectors (major and minor). Aggregation of the 5-minute counts to hourly values are used to construct hourly fractions for each measurement station.

To apply a time distribution for the FFCO₂ onroad emissions on each road segment, an Inverse Distance Weighting (IDW) spatial interpolation method was used. A search within a neighborhood of a 10 km radius is performed from the midpoint of each road segment to locate PeMS sites using a nearest neighbor searching library (Mount and Arya, 2010). In cases where more than one station was available, the IDW interpolation was applied; in cases where only one station was available, the time structure of this station was directly assigned to the road segment in question. In cases where no station was available within the 10-km neighborhood, an average temporal distribution was assigned (an average of all station values in a county at that hour for that road type). This last case occurred mostly in the rural portions of predominantly rural counties.

For local roads, PeMS data was not available in any of the counties within the Hestia-LA domain. Instead, the weekday hourly time fractions were generated from Annual Average Weekday Traffic (AAWT) data supplied by SCAG (Mike Ainsworth, 2014). The data contained five distinct time periods within a single 24 hour cycle: 6-9 am, 9 am-3 pm, 3-7 pm, 7-9 pm, 9 pm-6 am. Hourly time fractions for weekends were derived from the county average of weekend hourly time fractions. The weekday and weekend hourly time fractions were combined to form a complete week, and then replicated for all 52 weeks in the entire year. This was done because there was no significant seasonality in weekday and weekend traffic across the year as observed from PeMS data.

507 2.3.5 Nonroad

508 The nonroad Hestia-LA FFCO₂ emissions are completely determined in the Vulcan system and hence, passed to the
509 Hestia-LA domain without further processing (see Gurney et al., 2018 for details). To summarize the Vulcan
510 process, California did not report FFCO₂ nonroad emissions to the NEI 2011 but did report nonroad CO emissions.
511 The CO emissions were converted to FFCO₂ using the SCC-specific ratios of CO₂/CO derived from all other states
512 that reported both species (a mean value). The spatial distribution of the nonroad FFCO₂ emissions followed two
513 approaches. Nonroad FFCO₂ emissions reported through the 2011 NEI point data source (5 locations, 12% of
514 nonroad FFCO₂ in the LA Megacity) are located in space according to the provided latitude and longitude.
515 Emissions reported through the county-scale nonroad data source utilize multiple spatial surrogates provided by the
516 EPA reflecting a series of spatial entities such as the mines, golf courses and agricultural lands. There were instances
517 in which nonroad FFCO₂ emissions could not be associated with a spatial entity due to missing data. These
518 emissions are spatialized by first aggregating all the offending sub-county emission elements within a county for a
519 given surrogate shape type (e.g., golf courses, mines) and then distributing these emissions evenly across the county.
520 To distribute the nonroad FFCO₂ emissions from the annual to hourly timescale, a series of surrogate time profiles
521 provided by the EPA are used. These temporal surrogates are comprised of three cyclic time profiles (diurnal,
522 weekly, monthly) specific to SCC that are combined to generate hourly SCC-specific time fractions for an entire
523 calendar year.

524 2.3.6 Airport

525 Emissions of FFCO₂ from airports retrieved from the Vulcan system for the Hestia-LA domain are specific to
526 geocoded airport locations. Hence, the Hestia-LA system performs the temporal distribution only. There are 374
527 commercial airports/helipads in the Hestia-LA domain totaling 0.77 MtC/year, dominated by Los Angeles County
528 (0.39 MtC/year), and LAX in particular.
529 The annual airport FFCO₂ emissions are distributed in time utilizing airport-specific flight volume data from four
530 datasets:
531 1) The Operations Network (OPSNET) data from the Federal Aviation Administration (FAA) which reports total
532 date-specific, daily flight volume (365 values) at specific airports for specific aircraft classes (FAA, 2018a);
533 2) "AIRNAV" data which reports average daily percentage flight volume for aircraft class at US airports and
534 facilities (Aimav.com, 2018);
535 3) The Enhanced Traffic Management System Counts (ETMSC) daily flight volume data from the FAA was for two
536 airports in the Hestia-LA domain (NTD and RIV) with mostly military operations (FAA, 2018b);
537 4) The Los Angeles World Airports (LAWA) data which reports hourly flight volume for Los Angeles International
538 airport (LAX), Ontario airport (ONT), and Van Nuys airport (VNY) (LAWA, 2014).
539 For three large airports (LAX, ONT, VNY), the daily aircraft class-specific flight volume (from OPSNET) and the
540 hourly data on flight volume (from LAWA) were combined to create hourly aircraft class-specific time profiles

(Figure 4-6). All of the flight volume data are specific to four aircraft classes: Military (MIL), Air Carrier (AC), General Aviation (GA), and Air Taxi (AT).

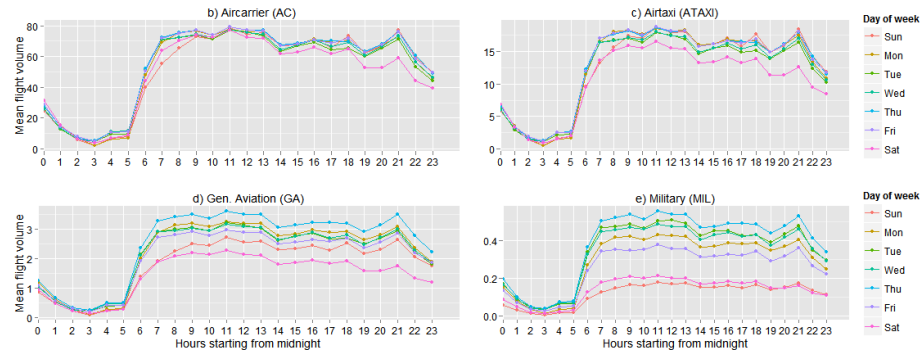


Figure 4. Average hourly flight volume at LAX for a) total, b) AC, c) AT, d) GA, and e) MIL aircraft classes for each day of the week. The plots represent the mean diurnal cycle for all Mondays, Tuesday, Wednesdays, and so on, given a full year of data.

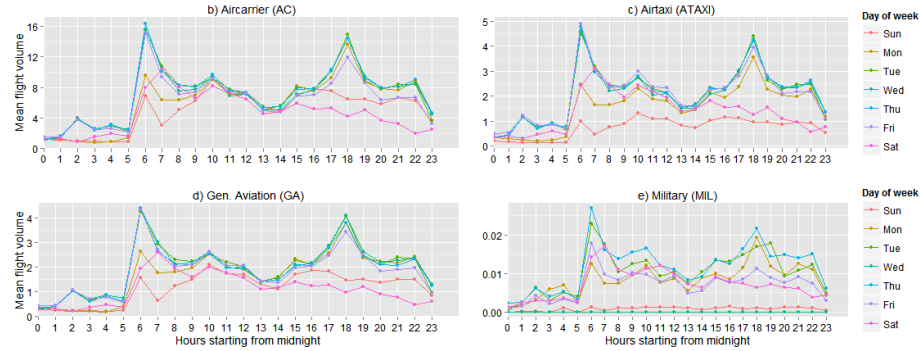


Figure 5. Same as figure 4 but for the Ontario (ONT) airport.

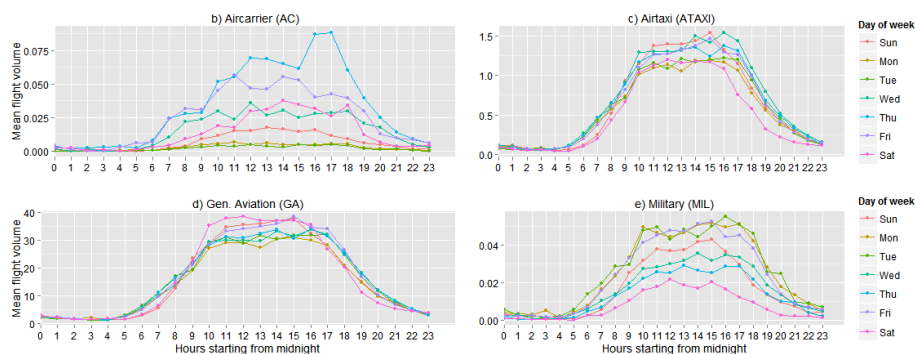


Figure 6. Same as figure 4 but for the Van Nuys (VNY) airport.

To generate hourly time profiles for all other airports in the Hestia-LA domain for which this type of detailed hourly data was not available, airports first were categorized based on average daily flight volumes and average aircraft class proportions from the OPSNET, AIRNAV and ETMSC data. Each airport was categorically matched to one of the two non-international airports with hourly data (ONT, VNY) and the hourly time fractions adopted. LAX was unique in terms of its volume and aircraft class proportions and hence was not used for any other airports. For helipads and very small airports, a flat time structure was used.

2.3.7 Railroad

Railroad FFCO₂ emissions are similarly distributed in space within the Vulcan system and passed through to the Hestia-LA landscape without alteration (see Gurney et al., 2018 for additional details). The Vulcan process treats railroad point records somewhat differently from the railroad nonpoint records. The point source railroad emissions are associated with rail yards and related geo-specific locales and are placed in space according to the provided latitude and longitude. The railroad FFCO₂ emissions associated with the nonpoint 2011 NEI reporting contain an ID variable that links to a spatial feature (rail line segment) in the EPA railroad GIS Shapefile. Nearly two-thirds of the railroad emitting segments have no segment link. The sum of these “unlinked” railroad FFCO₂ emissions are distributed to rail line within the given county according to freight statistics. The annual railroad FFCO₂ emissions are distributed to the hourly timescale with no additional temporal structure (a “flat” time distribution).

2.3.8 Commercial marine vessels

The commercial marine vessel (CMV) FFCO₂ emissions retrieved from the Vulcan system are specific to county and SCCs which are subsequently aggregated by the Hestia-LA system into emissions associated with two activity categories: “port” emissions “underway”. For the port CMV emissions (Figure 7), a port Shapefile from the EPA was used as a reference along with a visual inspection of the coastline (USEPA, 2015a).



Figure 7. The 6 ports in the Hestia-LA domain to which Vulcan FFCO₂ port emissions are allocated.

Allocation of the FFCO₂ emissions designated as “underway” used a polyline Shapefile (Figure 8) of commercial shipping lanes in California provided by CARB (Alexis, 2011). The shipping lanes for each county were bounded so that only lanes between the exterior of ports and a distance of 24 miles from the port exterior, were included. County total FFCO₂ emissions were then distributed evenly to these shipping lanes on a per unit length basis individually for each of the three counties. Each shipping lane segment receives its length fraction of the annual total of underway emissions.

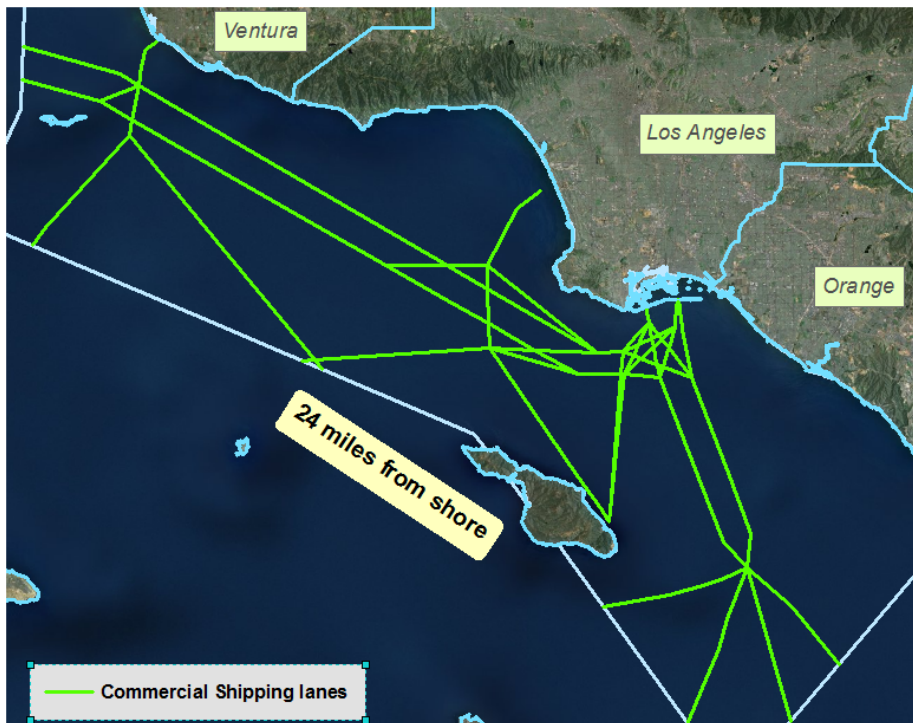


Figure 8. Commercial Marine Vessel (CMV) shipping lanes in the Hestia-LA to which Vulcan FFCO₂ underway emissions are allocated.

The time profile was based on the Marine Emissions Model (MEM) developed by CARB. MEM had marine vessel activity data which includes the arrival time of ocean-going vessels for all ports in California spanning the 2004 to 2006 time period (Alexis, 2011). This hourly dataset was analyzed using a Fourier time series which allowed for an isolation of the dominant cycles of ship traffic in the data. Results from the Fourier fit were then used to fill in the missing hours. Weekday hours were examined separately from weekend hours to isolate potential differences in traffic volume. Three cycles resulted: a 24-hour diurnal cycle, a weekly cycle and a monthly cycle. These were applied to all years of the annual FFCO₂ emissions to create an hourly distribution at each of the CMV ports within the domain.

2.3.9 Cement

Emissions of FFCO₂ from cement production facilities retrieved from the Vulcan system for the Hestia-LA domain are specific to geocoded facility locations. CO₂ is emitted from cement manufacturing as a result of fuel combustion and as process-derived emissions [van Oss, 2005]. The emissions from fuel combustion are captured in the industrial sector. The process-derived CO₂ emissions result from the chemical process that converts limestone to calcium

oxide and CO₂ during “clinker” production (clinker is the raw material for cement which is producing by grinding the clinker material). These emissions are reported as cement sector emissions. These emissions are fully calculated, spatialized and temporalized in the Vulcan v3.0 system and passed directly to the Hestia-LA landscape. The cement facilities are geocoded with some corrections to provide more accurate placement of the emission stacks.

2.4 Gridding

The county-level FFCO₂ emissions inventory, which has been distributed into the point, line and polygon features by sector, are rasterized into a sector-specific and time-resolved gridded form under a common grid reference. This grid reference divides the entire Hestia-LA domain into 509-by-342 1 km x 1 km grid cells on the California State Plane Coordinate System. The grid reference is made into “fishnet” in the Shapefile format with 509-by-342 square geometries.

The first step of the gridding procedure is to perform a spatial intersection operation between the fishnet and each of the sectoral emissions layers in ArcGIS. The output of an intersection operation is a new set of features common to both input layers. The emissions value of each feature in the intersection output was scaled by the ratio of the spatial footprint of the feature to that of the original feature in the sectoral emissions layer. For line-source and polygon-source emissions layers, the spatial footprint represents the line length and polygon area respectively. For point-source layers, the footprint is equal to 1.

2.5 Uncertainty

Uncertainty estimation for Hestia results are challenging owing to the fact that many of the datasets used to construct the flux results are not accompanied by uncertainty or traceable to transparent sources or methods. The approach taken for the Hestia-LA v2.5 results was to conservatively estimate the uncertainty based on available comparisons to Hestia results and exploration of the dominant components of the Hestia output. The first of these is a comparison of the Hestia-Indianapolis (Hestia-Indy) results to an inverse-estimation of fluxes in the INFLUX project (Gurney et al., 2017). In that study, it was shown that the Hestia-Indy whole-city FFCO₂ emissions result agreed with an inverse estimate (Lauvaux et al., 2016) within 3.3% (CI: -4.6% to +10.7%). This suggests both potential bias (3.3%) and an estimation uncertainty (~7.5%). This comparison was accomplished by estimating portions of the carbon budget, included in the inverse estimate, but not explicitly included in the Hestia-Indy result. Most importantly, biosphere respiration estimated from chamber studies at commensurate urban latitudes combined with a remote-sensing based approach to quantifying the available vegetated landscape. This comparison, it should be noted, is for a single city (Indianapolis) for a single time period. We directly sum the random and systematic error and use this in the current study to represent the Hestia-LA whole-city uncertainty (a 95% CI), rounded up to 11%. The next element for consideration with a conservative uncertainty estimate is the work done to compare two different electricity production FFCO₂ estimates in the US. This work (Gurney et al., 2016) found that one-fifth of the facilities had monthly FFCO₂ emission differences exceeding -6.4%/+6.8% for the year 2009 (the closest analyzed year to the 2011 analysis examined here). The distributions of emissions of the two datasets were not

631 normally distributed nor were the differences. Hence, a typical gaussian uncertainty estimate cannot be made –
 632 rather, the difference distribution was represented by quintiles of percentage difference. Hence, these values cannot
 633 be cast within the context of other normally-distributed errors. However, we conservatively consider the quintile
 634 value (the positive and negative tails) as a one-sigma value and 13% as a two-sigma value. The contribution of
 635 electricity production is important to urban FFCO₂ emissions uncertainty given how large power production can be
 636 within the total urban FFCO₂ context. For example, in the Los Angeles Megacity electricity production accounts for
 637 19% of the total FFCO₂ emissions. The percentage differences can act as a form of uncertainty at the pointwise or
 638 (conservatively) the gridcell scale, though only representative of the type of uncertainties represented by electricity
 639 production point sources.
 640 Finally, an initial assessment of the range of two critical parameters in the Vulcan/Hestia estimation is included as
 641 part of the conservative uncertainty estimation. The two critical parameters are the CO emissions factor and the CO₂
 642 emissions factor. Primarily for the CO EF, there is a range of potential values for each application (combination of
 643 fuel category and combustion technology) though that range is not represented by a well-populated distribution of
 644 values, but rather a discrete set of values within the data sources described in Gurney et al. (2009). Furthermore, the
 645 expectation is that the CO EFs would not be normally distributed even were there to be a well-populated distribution
 646 of values (i.e. many literature estimates of the same fuel/combustion technology) owing to the nature of CO
 647 emissions from fuel combustion. This is driven by both the variation in combustion conditions for a given
 648 fuel/technology combination and the variation in CO EF values across combustion technology. The distribution
 649 would likely be a positively skewed “heavy” or “long” tailed distribution. For the current study, a range of the CO
 650 and CO₂ EF values culled from the literature are conservatively assigned a one-sigma uncertainty of 10% or a two-
 651 sigma value of 20%. Like the electricity production analysis in the previous paragraph, the uncertainty associated
 652 with the CO and CO₂ emission factors is a gridcell-scale uncertainty (as opposed to whole city where error
 653 cancelation occurs) and is independent of the electricity production uncertainty estimate (the CO and CO₂ EF values
 654 are not used in the electricity production sector but in the other point sources and nonpoint sources).
 655 These latter two uncertainty are more representative of gridcell-scale uncertainties and sum them in quadrature to
 656 arrive at a gridcell-scale uncertainty (95% CI) of 23.4% or conservatively rounded to 25%. Work is underway that
 657 includes a complete input parameter range for the Hestia emissions data results to more formally assign uncertainty
 658 at multiple scales.

659 3 Results

660 The total 2011 emissions for the Hestia-LA domain are 48.06 ± 5.3 MtC/yr (Figure 9, Table 5). Transportation
 661 accounts for the largest share (24.27 ± 2.7 MtC/yr) of the total and within the transportation sector, onroad emissions
 662 account for the largest portion (20.81 ± 2.3 MtC/yr). The next largest sectors are the industrial (11.65 MtC/yr ± 1.3)
 663 and electricity production (5.88 ± 0.76 MtC/yr) sectors, respectively. Onroad, electricity production, residential and
 664 industrial FFCO₂ emissions make up 86% of the total. Petroleum accounts for almost 75% of the total LA Megacity
 665 fuel consumption for direct FFCO₂ emissions consistent with the dominance of the transportation and industrial

sectors which are mostly reliant on petroleum fuels. Los Angeles County dominates emissions in the five counties of the Hestia-LA domain accounting for 55% of the total FFCO₂ emissions. This is followed by San Bernardino, Orange, Riverside, and Ventura counties, respectively. Los Angeles and San Bernardino counties are dominated by onroad and industrial FFCO₂ emissions, while onroad emissions account for the largest share, by far, in the remaining three counties. Not surprisingly, Los Angeles county has the largest CMV FFCO₂ emissions among the five counties owing to the port of Los Angeles which hosts a large amount of international commercial shipping. At 0.61 ± 0.067 MtC/yr, it rivals in emission magnitude the combination of residential and commercial building emissions in each of the other four counties.

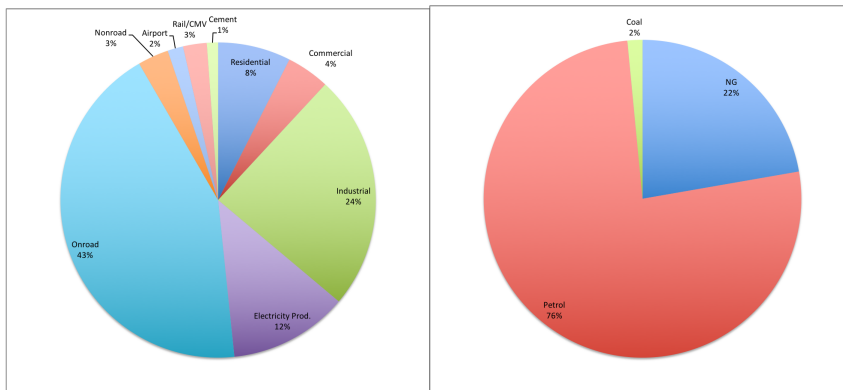


Figure 9. Total FFCO₂ emissions proportions for the Hestia-LA domain. a) FFCO₂ emission proportions by sector; b) FFCO₂ emission proportions by fuel category.

Table 5. Sectoral FFCO₂ emissions in the five Hestia-LA domain counties for the year 2011. Units: MtC/yr.

| Sector | Los Angeles (MtC/yr) | Orange (MtC/yr) | San Bernardino (MtC/yr) | Riverside (MtC/yr) | Ventura (MtC/yr) | Total (MtC/yr) |
|------------------------|-------------------------|--------------------|----------------------------|-----------------------|---------------------|-------------------|
| Residential | 2.00 | 0.64 | 0.40 | 0.36 | 0.20 | 3.59 |
| Commercial | 1.47 | 0.12 | 0.21 | 0.24 | 0.071 | 2.12 |
| Industrial | 7.27 | 0.94 | 2.99 | 0.25 | 0.20 | 11.65 |
| Electricity production | 2.73 | 0.69 | 1.54 | 0.71 | 0.21 | 5.88 |
| Transportation | 12.95 | 3.83 | 3.58 | 2.88 | 1.02 | 24.27 |
| Onroad | 11.03 | 3.46 | 2.98 | 2.51 | 0.82 | 20.81 |
| Nonroad | 0.79 | 0.27 | 0.19 | 0.19 | 0.087 | 1.52 |
| Airport | 0.39 | 0.06 | 0.14 | 0.11 | 0.070 | 0.77 |
| Railroad | 0.13 | 0.028 | 0.27 | 0.072 | 0.010 | 0.51 |
| CMV | 0.61 | 0.012 | 0 | 0 | 0.037 | 0.66 |
| Cement | 0 | 0 | 0.55 | 0.0077 | 0 | 0.55 |
| Total | 26.42 | 6.22 | 9.28 | 4.45 | 1.70 | 48.06 |

Total emissions in the LA Megacity show a small downward trend over the 2010-2015 time period of 0.44%/year which is a statistically significant trend (slope: -0.21 MtC/yr; CI: -0.397, -0.023). Individual sectors show greater variation there are compensating temporal changes among the individual sectors (Figure 10). The residential sector showed a relatively large decline in 2014, though due to its relatively small portion of total emissions, has limited impact on the total temporal variation from 2010-2015. Similarly, 2015 showed a large increase in commercial

sector emissions which also do not translate to large changes in the total FFCO₂ emissions time series. The relative temporal stability of the industrial and onroad FFCO₂ emissions sectors combined with their large share of the total FFCO₂ emissions are reflected in the total emissions trend. When categorized by fuel type, natural gas FFCO₂ emissions exhibited the greatest variation with a maxima in 2012 and to a lesser extent 2013, driven primarily by consumption in the electricity production sector.

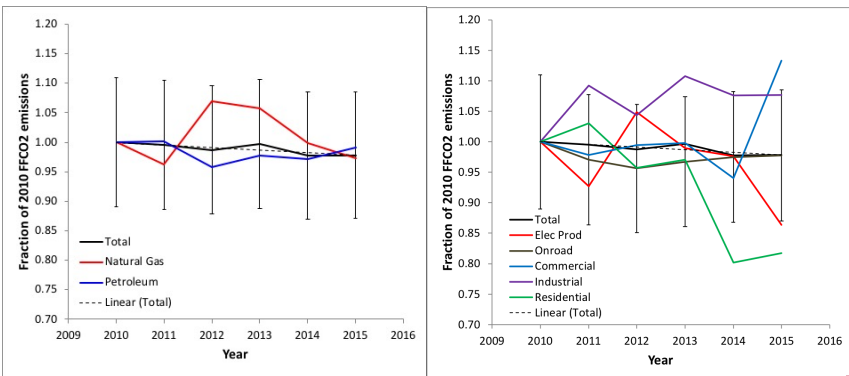
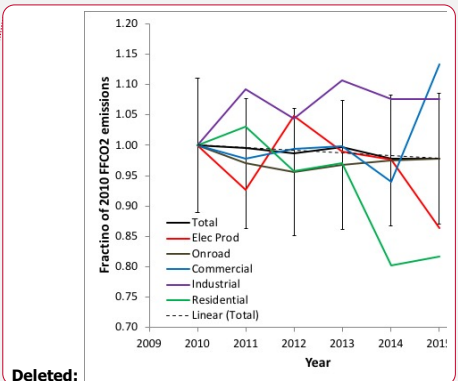


Figure 10. Fractional changes over the 2010 to 2015 timeframe in LA Basin FFCO₂ emissions. a) by fuel category; b) by sector. Whole-city error provided for the total FFCO₂ emissions only.

Spatial distribution of the Hestia-LA FFCO₂ emissions demonstrate the importance of the populated areas and road-intensive portions of the domain in the overall emissions (Figure 11). The constant emissions that appear over large areas, particularly in San Bernardino and Riverside counties, are due to the nonroad FFCO₂ emissions which have relatively simple spatial distribution proxies with considerable areal extent.



Deleted:

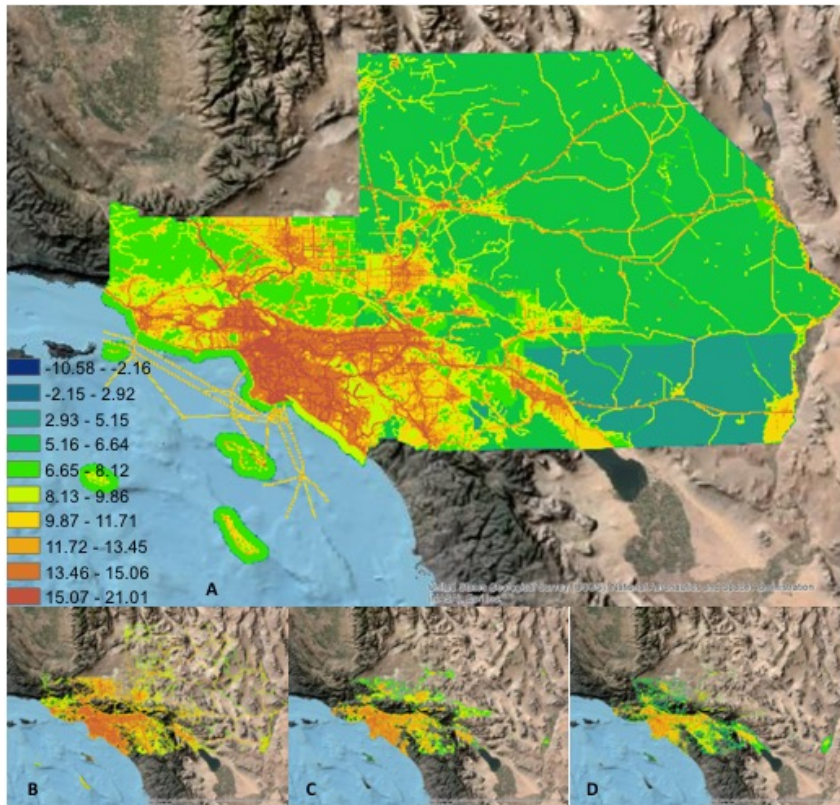


Figure 11. Hestia-LA v2.5 FFCO₂ emissions for the year 2011 represented on a 1 km x 1 km grid. a) total FFCO₂ emissions; b) onroad FFCO₂ emissions; c) residential FFCO₂ emissions; d) commercial FFCO₂ emissions. Units: natural logarithm KgC/gridcell/yr.

Figure 12 shows the cumulative FFCO₂ emissions across four of the sectors for which the 1 km² gridcell accumulation is most appropriate: the commercial, industrial, onroad, and residential sectors. The other FFCO₂ emission sectors (airport, electricity production, cement) are not included in Figure 12 because they are dominated by a few points, have limited spatial distribution (railroad) or no spatial variance (nonroad). The accumulation of FFCO₂ emissions at the threshold by which 10% of the gridcells are accumulated is noted on the figure. For the industrial sector, 10% of the largest emitting gridcells account for 93.6% of the total industrial sector emissions. For the commercial sector this occurs at 73.4% of the accumulated gridcells. For the onroad and residential sectors this occurs at 66.2% and 45.3%, respectively. This demonstrates two important points about the FFCO₂ emissions in the Los Angeles Megacity (and most cities). First, the emissions have very high spatial variance with few gridcells accounting for a large portion of the total FFCO₂ emissions. Second, this is particularly true for the industrial sector, driven by the fact that it is comprised of a large proportion of point emitters. This is somewhat true of the

commercial sector which does have some pointwise data within the original NEI reporting. Of the remaining two sectors, which contain no pointwise spatial emitters, the majority (66.2%) of the onroad emissions are captured in the largest 10% while the residential sector, being less concentrated, shows an accumulation just short of the 50% threshold at a 10% gridcell accumulation threshold.

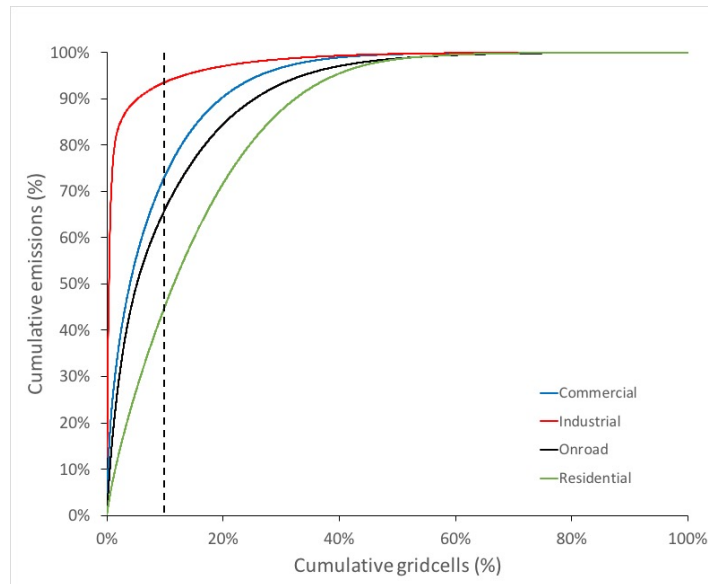


Figure 12. Cumulative FFCO₂ emissions according to key sectors in the Hestia-LA FFCO₂ emissions data product. The dashed line at 10% cumulative grid cells is given for reference. See text for details.

An important attribute of estimating urban emissions at fine space and time scales is the resulting clustering in space (and time) of the emissions and the varying patterns of the clustering across the emitting sectors. Figure 13 provides an analysis of spatial clustering using the *Getis-Ord-Gi* statistic which provides a score that measures statistically significant departures from random local clustering (*Getis and Ord, 1992*). The three sectors included in this analysis are the residential, commercial and onroad sectors. The onroad sector shows a more widely dispersed clustering pattern with local “hotspots” generated by high traffic flow points and traffic congestion, primarily on the interstate network coincident with a greater density of commercial and residential activity. The residential sector exhibits less extensivity compared to the onroad FFCO₂ emissions clustering but with larger individual hotspot areas. Particularly large clustering occurs from the coast centered on Santa Monica and Marina del Rey and extending East and North through West Hollywood on to Pasadena and Alhambra. Other hotspots occur in the Manhattan Beach to Redondo Beach corridor, the Burbank and Glendale area and the coastal portion of Orange county (e.g. Huntington Beach, Newport Beach). The commercial sector shows the a similar overall extensivity to the residential sector but with less extensive individual hotspots associated with commercial building clusters.

nonroad sector in the onroad category as the SCAG inventory did not explicitly include a nonroad sector. SCAG documentation suggests that the nonroad sector is included in the forecasts for the residential, commercial and industrial sectors (SCAG, 2012, page C-10) but further details on the base year estimates could not be found and no mention is made in the report where these sectors are described. If the Hestia nonroad estimate (1.56 MtC/yr) were not allocated to onroad but distributed to the residential, commercial and industrial sectors it would exacerbate the difference in the onroad, commercial and industrial sectors.

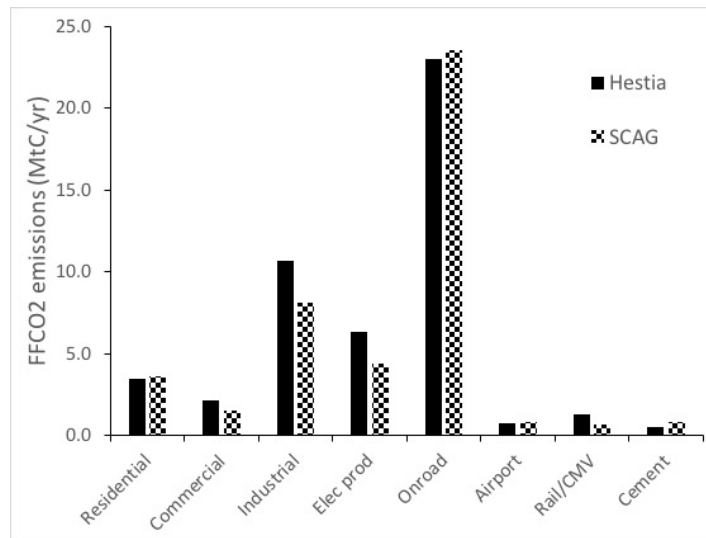


Figure 14. Comparison of sector-specific FFCO₂ emissions for the year 2010 between the Hestia-LA and SCAG estimates. Units: MtC/yr.

The California Energy Commission archives energy consumption data for both natural gas and electricity (<http://ecdms.energy.ca.gov/>). The data is archived as specific to the residential sector and the non-residential sector. Because of ambiguities regarding the non-residential sector definition, we compare the reported values by county for the residential only (Table 6). Good agreement for natural gas FFCO₂ emissions is achieved for the Los Angeles Megacity as a whole (<1%) with some variation at the scale of the individual counties. Agreement with the CEC estimate is better than that found for the comparison with the SCAG inventory (Hestia being 3.1% lower than the SCAG residential NG FFCO₂ estimate).

Table 6. Residential natural gas FFCO₂ emissions in the five Hestia-LA domain counties for the year 2011 compared to estimates from the California Energy Commission (CEC). Units: MtC/yr.

| County | Hestia | CEC | diff (%) |
|----------------|--------|------|----------|
| Los Angeles | 1.94 | 1.98 | -2.0% |
| Orange | 0.63 | 0.59 | 5.7% |
| San Bernardino | 0.40 | 0.39 | 0.8% |
| Riverside | 0.35 | 0.39 | -11.1% |
| Ventura | 0.19 | 0.18 | 6.5% |

| | | | |
|-------------|------|------|-------|
| LA Megacity | 3.51 | 3.54 | -0.9% |
|-------------|------|------|-------|

772 Average hourly variations in FFCO₂ emissions are sensitive to both the sector and spatial location. Figure 15
 773 presents annual mean diurnal patterns specified by county and sector (the railroad or cement sectors were
 774 constructed with no diurnal cycle and hence is not shown). As noted previously, Los Angeles county shows the
 775 greatest emissions overall, particularly for the commercial marine vessel sector where the port of Los Angeles
 776 dominates. The commercial, residential, onroad and CMV sectors exhibit two maxima, one in the morning (~5-10
 777 am, local time) and another in the afternoon/evening. In the commercial sector, this afternoon/evening maximum
 778 occurs later in this time period centered on 9 pm local time, coinciding with retail closing schedules. The maximum
 779 CMV emissions are shifted by roughly two hours earlier in the day for both the morning and afternoon/evening
 780 peaks. The afternoon/evening maximum for the onroad sector shows an afternoon/evening maximum that is of
 781 longer duration than that in the morning with emissions gradually rising after the midpoint of the day, local time. In
 782 addition to large daily variations, the onroad sector contains a significant weekly temporal pattern with emissions
 783 largest on Monday and smallest on Saturday (Figure 16).

784 Diurnal patterns in onroad and airport FFCO₂ emissions have a single maximum at the middle of the day but broadly
 785 extending across all daylight hours. In the case of the nonroad emissions, this is simply a reflection of the EPA
 786 temporal surrogate applied. In the case of the airport FFCO₂ emissions, the time structure reflects the reported air
 787 traffic volume at the major airports in the LA Megacity. Finally, the industrial and electricity production sectors
 788 maintain relatively constant emissions across all 24 hours. In the case of the industrial sector, this reflects the
 789 integration of industry-specific EPA temporal surrogates within a given county. For the electricity production sector,
 790 the time structure is primarily driven by the stack-monitored emissions and shows a slightly greater emission in the
 791 evening hours compared to all other hours.

792 The diurnal patterns are consistent across all five counties with the exception of the commercial sector where there
 793 are small differences in the maximum point of the morning emissions in San Bernardino and Ventura counties
 794 compared to the other LA Megacity counties.

795

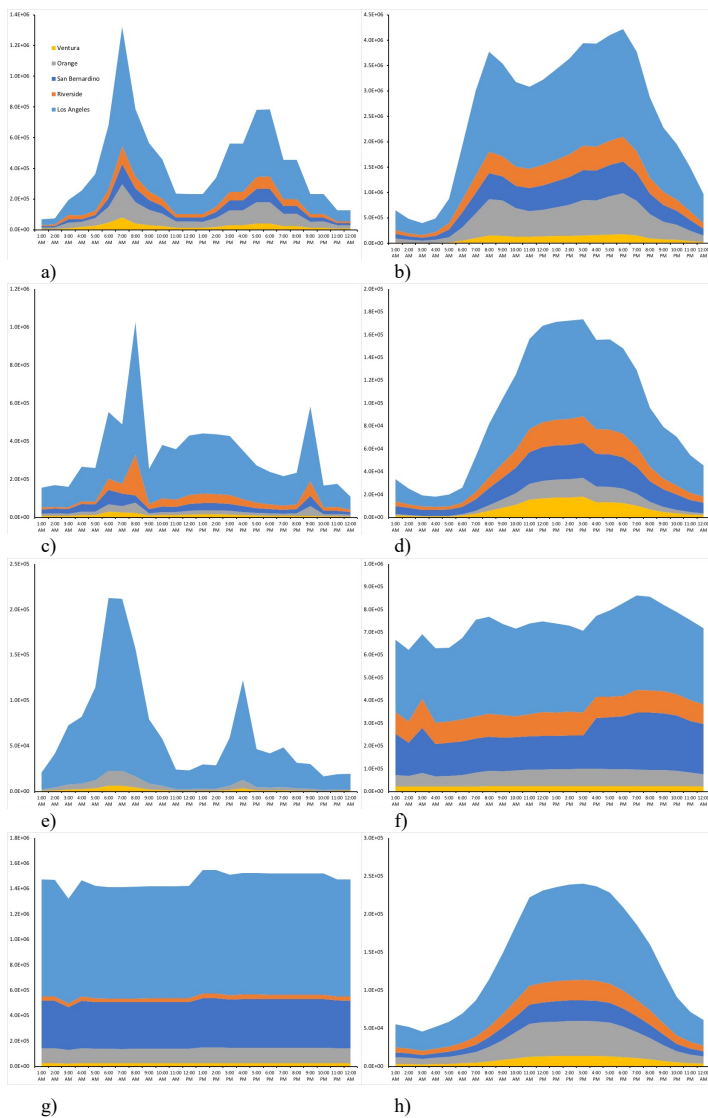


Figure 15. Average daily FFCO₂ emissions in the Hestia-LA v2.5 data product for five counties across eight sectors. A) residential; b) onroad; c) commercial; d) airport; e) commercial marine vessel; f) electricity production; g) industrial; h) nonroad. Note: different scale range on each plot. Units: kgC/hour.

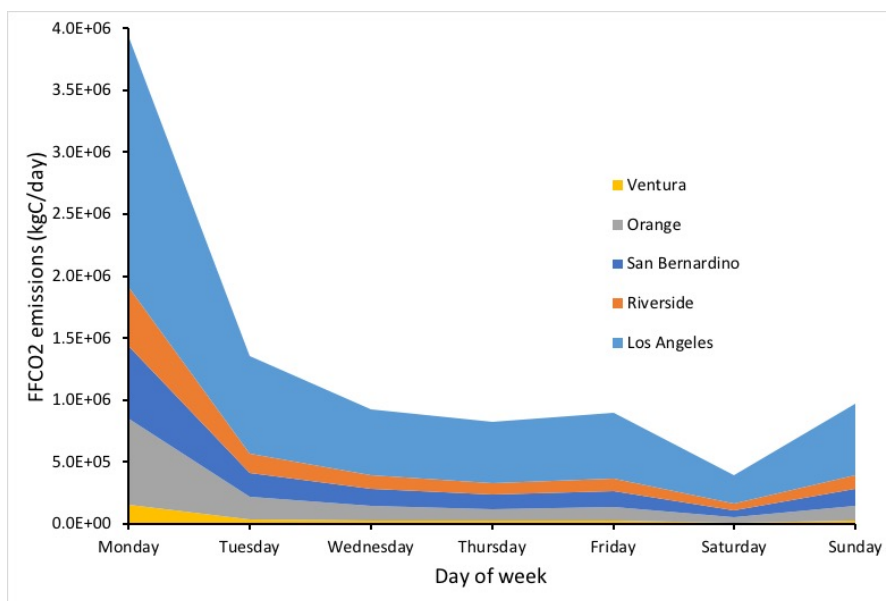


Figure 16. Average weekly onroad FFCO₂ emissions from the Hestia-LA v2.5 data product for five counties. Units: kgC/day

4 Discussion

The first Hestia urban FFCO₂ emissions data product was produced for the Indianapolis domain (Gurney et al., 2012). As an outcome of the Hestia effort, a large multifaceted effort, the Indianapolis Flux Experiment (INFLUX), emerged (Whetstone et al., 2017; Davis et al., 2017). INFLUX aims to advance quantification and associated uncertainties of urban CO₂ and CH₄ emissions by integrating a high-resolution bottom-up emission data product, such as Hestia, with atmospheric concentration measurements (Turnbull et al., 2015; Miles et al., 2017; Richardson et al., 2017), flux measurements (Cambaliza et al., 2014; 2015; Heimberger et al., 2017), and atmospheric inverse modeling. In addition to its use as a key constraint in the INFLUX atmospheric inverse estimation (Lauvaux et al., 2016), Hestia has been informed by atmospheric observations making it useable as a standalone high-resolution flux estimate offering a detailed space-time understanding of urban emissions. Begun in the late 2000s, INFLUX has explored many aspects of the individual elements of a scientifically-driven urban flux assessment (e.g. Wu et al., 2018) in addition to demonstrating potential reconciliation between Hestia and the atmospheric measurements (Gurney et al., 2017; Turnbull et al., 2018). Similar efforts are ongoing in the Salt Lake City (Mitchell et al., 2016; Lin et al., 2018) and Baltimore (Martin et al., 2018) domains with a different arrangement of atmospheric monitoring and modeling. As with INFLUX, a Hestia FFCO₂ emissions data product was produced in each domain (Patarasuk et al., 2016; Gurney et al., 2018).

827 The Hestia Los Angeles Megacity effort was developed under the Megacities Carbon Project framework
 828 (<https://megacities.jpl.nasa.gov/portal/>). It was designed to serve the Megacities Carbon Project in a similar capacity
 829 to its role in INFLUX. The Hestia-LA results are unique in that it is the first high-resolution spatiotemporally-
 830 explicit inventory of FFCO₂ emissions centered over a megacity. Presented here at the 1 km² spatial and hourly
 831 temporal resolution, the emissions can be represented at finer spatial scales down to the individual building, though
 832 with higher uncertainty. While policy emphasis in California thus far has been focused on CH₄ emissions (Carranza
 833 et al., 2017; Wong et al., 2016; Verhulst et al., 2017; Hopkins et al., 2016), work is ongoing to use the extensive
 834 atmospheric CO₂ observing capacity in the Los Angeles domain (e.g. Newman et al., 2016; Wong et al., 2015;
 835 Wunch et al., 2009) within an atmospheric CO₂ inversion. This will offer an important evaluation of the Hestia-LA
 836 emissions for which limited independent evaluation is currently available.

837 The potential of the Hestia-LA FFCO₂ emissions to enable or assist with policymaking in the cities, counties or
 838 metropolitan planning domain of the overall Southern California area is considerable. The traditional urban
 839 inventory approach, such as accomplished by many cities as part of their climate action plans, are whole-city
 840 accounts, often specific to sector, that follow one of a few inventory protocols. Given the challenges of data
 841 acquisition and the idiosyncrasies of protocol choice and needs, the traditional urban inventories are difficult to
 842 compare across cities and hence, aggregate reliably in a metropolitan domain such as the LA Megacity. Importantly,
 843 without space and time explicit emissions information, they are difficult to calibrate with atmospheric measurements
 844 and hence, evaluate against this important scientific constraint. The Hestia-LA FFCO₂ emissions approach attempts
 845 to overcome these limitations to traditional inventory work. By quantifying emissions at the scale of individual
 846 buildings and road segments, with process detail such as the sector, fuel, and combustion technology, Hestia results
 847 can be organized according to most of the protocols in use by cities. This explicit space and time detail also allow
 848 for calibration to atmospheric measurements, for which emission location and time structure is essential.

849 The state of California continues to lead the nation in climate policy with numerous legislative and executive orders
 850 outlining both general reduction goals and specific policy instruments. The California Global Warming Solutions
 851 Act (Assembly Bill 32) passed in 2006, specifies a statewide reduction in greenhouse gas emissions to 1990 levels
 852 by the year 2020 (<https://www.arb.ca.gov/cc/ab32/ab32.htm>). Furthermore, the bill requires reporting and
 853 verification of reductions in order to demonstrate compliance. Executive order B-30-15 and Senate Bill, SB 32 have
 854 built on this with an aim to reduce emissions 40% below 1990 levels by 2030 and 80% below 1990 levels by 2050,
 855 respectively (<https://www.gov.ca.gov/2015/04/29/news18938/>;
 856 https://leginfo.ca.gov/faces/billTextClient.xhtml?bill_id=201520160SB32). Ultimately, much of the
 857 specific action needed to meet these goals will rest upon local governments and authorities. Given that 87% of the
 858 state population resides in urban areas and nearly half of state population resides in the Los Angeles Megacity, the
 859 cities and counties that comprise the Los Angeles metropolitan area have a central role to play in achieving the
 860 statewide climate change policy goals. The city of Los Angeles, the largest individual city in the metro region, has
 861 specified goals consistent with the state commitments, expecting to reduce greenhouse gas emissions 35% below
 862 1990 levels by the year 2030 (http://environmentla.org/pdf/GreenLA_CAP_2007.pdf). To meet these reduction

863 goals, policy actions will become increasingly difficult to achieve at no- or low-cost and economic efficiency will
864 become central to making policy choices.

865 The most important attribute of the Hestia-LA approach, therefore, is the potential it offers for targeting urban CO₂
866 reduction policy more efficiently. As shown in Figures 12 and 13, FFCO₂ emissions are highly variable in space and
867 typically cluster in concentrated areas. In choosing specific policy approaches and instruments, this offers Los
868 Angeles policymakers the ability to target specific neighborhoods, road segments, or commercial hubs, where
869 policies will achieve the greatest reduction for resources expended. This rests on the argument that specificity leads
870 to efficiency. As all cities, including those in the Los Angeles Megacity, move towards those aspects of carbon
871 emission reductions that are not part of the “low hanging fruit” policy instruments, competition for limited resources
872 and policy justification will increase. Having information that targets the most efficient and effective emission
873 reduction investments, established by independent rigorous scientific information, will be at a premium. For
874 example, if a small proportion of the commercial sector buildings in the LA Megacity account for a large proportion
875 of the FFCO₂ emissions, knowing the location of these buildings and targeting energy efficiency programs to those
876 buildings, may offer the most economically efficient route to emissions reductions in the commercial sector. A
877 similar argument can be made in the onroad sector due to the clustering of large onroad emitting gridcells and
878 specific road-class attributes (see Rao et al., 2017).

879 A number of caveats are worth mentioning in association with the Hestia-LA v2.5 FFCO₂ emissions results. With
880 Vulcan v3.0 as the starting point for the quantification in Hestia, errors in Vulcan will be passed to Hestia, with a
881 few exceptions. Of particular note are the industrial sector and more specifically, refining operations which have
882 limited emissions reporting. These remain difficult to quantify due to the range of CO emission factors representing
883 many of the combustion processes undertaken at these large and complex facilities. The uncertainty estimation
884 described remains limited and there are additional sources of uncertainty that must be quantified such as categorical
885 errors (e.g. mis-specification of fuel category or road class), errors in spatial accuracy and spatial error correlation.
886 Quantifying these contributions to the overall uncertainty presented here remain a task for future work.

887 **5 Data availability, policy and future updates**

888 The Hestia-LA v2.5 emissions data product can be downloaded from the data repository at the National Institute
889 of Standards and Technology (<https://doi.org/10.18434/T4/1502503>) and is distributed under Creative Commons
890 Attribution 4.0 International (CC-BY 4.0, <https://creativecommons.org/licenses/by/4.0/deed.en>). The Hestia-LA
891 v2.5 FFCO₂ emissions data product is provided as annual and hourly (local and UTC versions) 1 km x 1 km
892 NetCDF file formats, one file for each of the 6 years (2010-2015). The hourly files are approximately 2.9 GB each.
893 The annual files are 0.34 GB each.
894 Attempts will be made to update the Hestia-LA FFCO₂ emissions on a roughly bi-annual basis, depending upon
895 support, the availability of updates to the Vulcan FFCO₂ emissions data product, and updates to the additional data
896 sources described in this study.

897 6 Conclusion

898 The Hestia Project quantifies urban fossil fuel CO₂ emissions at high space- and time-resolution with application to
899 both scientific and policy arenas. We present here the Hestia-LA version 2.5 FFCO₂ emissions data product which
900 represents hourly, 1 km², sector-specific emissions for the five counties of the Los Angeles metropolitan area for the
901 2010 to 2015 time period. The methodology relies on the results of the Vulcan Project (version 3.0) further
902 enhancing and distributing emissions to the scale of individual buildings and road segments with local data sources
903 acquired from local government agencies. Each sector is quantified using data sources and spatial/temporal
904 distribution approaches distinct to the sector characteristics. The results offer a detailed view of FFCO₂ emissions
905 across the LA Megacity and point to the extreme spatial variance of emissions. For example, 10% of the 1 km²
906 emitting gridcells account for 93.6%, 73.4%, 66.2%, and 45.3% of the emissions in the industrial, onroad,
907 commercial, and residential sectors, respectively. We find that the LA Megacity emitted 48.06 ± 5.3 MtC/yr in the
908 year 2011, dominated by Los Angeles county (26.42 ± 2.9 MtC/yr) and from a sector-specific viewpoint, dominated
909 by the onroad sector (20.81 ± 2.3 MtC/yr). Hestia FFCO₂ emissions are 10.7% larger than the inventory estimate
910 generated by the local metropolitan planning agency, a difference that is driven by the industrial and electricity
911 production sectors. Good agreement is found (<1%) when comparing residential natural gas FFCO₂ emissions to
912 utility-based reporting at the county spatial scale. The largest temporal variations are found in the diurnal cycle with
913 the residential, commercial, onroad, and commercial marine vessel emissions showing to maxima, one in the
914 morning and a second in the afternoon/evening. Airport and nonroad emissions, by contrast show broad maxima
915 across the daylight hours. Finally, the industrial and electricity production sectors show little diurnal variation across
916 24 hours. The onroad sector also exhibits variation in the weekly distribution of emissions with maximum FFCO₂
917 emissions on Monday and minimum emissions on Saturday.

918 The Hestia-LA v2.5 FFCO₂ emissions data product offers the scientific and policymaking communities
919 unprecedented spatially and temporally-resolved information on FFCO₂ emission sources in the Los Angeles
920 Megacity. As part of the Megacities Carbon Project, future work includes incorporation into atmospheric CO₂
921 inversion research to further evaluate the Hestia-LA data product and improve estimation. Policymakers can use the
922 Hestia-LA results to better-understand FFCO₂ emissions at the human scale, offering the potential for improved
923 targeting of FFCO₂ reduction policy instruments. Finally, urban researchers can use Hestia-LA to explore a number
924 of important urban science questions such as how emissions intersect with other urban sociodemographic variables
925 such as income, education, housing size, or vehicle ownership.

926 The Hestia-LA data product is publicly available and will be updated with future years as data becomes available.

927 **Competing Interests.** The authors declare that they have no conflict of interest.

928 **Acknowledgments.** This research was made possible through support from the National Aeronautics and Space
929 Administration Carbon Monitoring System program, Understanding User Needs for Carbon Information project
930 (subcontract 1491755), the National Aeronautics and Space Administration grant NNX14AJ20G, the National

931 Institute of Standards and Technology grant 70NANB14H321 and 70NANB16H264, JPL's Strategic
932 University Research Partnership program, and the Trust for Public Land.

933 References

- 934 Ainsworth, M. (2014) Shapefile with AAWT data. Retrieved by personal communication from Mike Ainsworth
935 (AINSWORT@scag.ca.gov) and Cheryl Leising (leising@scag.ca.gov) at Transportation Planning Department,
936 SCAG Riverside Office.
- 937 AirNav.com. Data retrieved from: <http://www.airnav.com/airports/> (Aug 1, 2018).
- 938 Alexis, A. (2011), Marine Emissions Model, California Air Resources Board. personal communication with Andy
939 Alexis, July 6, 2011 (email: aalexis@arb.ca.gov). Retrieved from:
940 <https://www.arb.ca.gov/ports/marinevess/ogv/ogv1085.htm>
- 941 Bréon, FM, Broquet, G, Puygrenier, V, Chevallier, F, Xueref-Remy, I, et al. 2015 An attempt at estimating Paris
942 area CO₂ emissions from atmospheric concentration measurements, *Atmos. Chem. Phys.*, **15**: 1707–1724.
943 <http://www.atmos-chem-phys.net/15/1707/2015/>, DOI: <https://doi.org/10.5194/acp-15-1707-2015>
- 944 Cambaliza, M. O. L., Shepson, P. B., Caulton, D. R., Stirm, B., Samarov, D., Gurney, K. R., Turnbull, J., Davis, K.
945 J., Possolo, A., Karion, A., Sweeney, C., Moser, B., Hendricks, A., Lauvaux, T., Mays, K., Whetstone, J.,
946 Huang, J., Razlivanov, I., Miles, N. L. and Richardson, S. J.: Assessment of uncertainties of an aircraft-based
947 mass balance approach for quantifying urban greenhouse gas emissions, *Atmos. Chem. Phys.*, **14**(17), 9029–
948 9050, doi:10.5194/acp-14-9029-2014, 2014.
- 949 Cambaliza, M. O. L., Shepson, P. B., Bogner, J., Caulton, D. R., Stirm, B., Sweeney, C., Montzka, S. a., Gurney, K.
950 R., Spokas, K., Salmon, O. E., Lavoie, T. N., Hendricks, A., Mays, K., Turnbull, J., Miller, B. R., Lauvaux, T.,
951 Davis, K., Karion, A., Moser, B., Miller, C., Obermeyer, C., Whetstone, J., Prasad, K., Miles, N. and
952 Richardson, S.: Quantification and source apportionment of the methane emission flux from the city of
953 Indianapolis, *Elem. Sci. Anthr.*, **3**, 37, doi:10.12952/journal.elementa.000037, 2015.
- 954 [California Air Resources Board \(2010\) Documentation of California's Greenhouse Gas Inventory, June 2010.](#)
955 [Retrieved from: <http://www.arb.ca.gov/cc/inventory/doc/doc.htm>](#)
- 956 California Air Resources Board (2014) *EMFAC2014 Volume I – User's Guide*, v1.0.7, April 30, 2014, California
957 Environmental Protection Agency Air Resources Board, Mobile Source Analysis Branch, Air Quality Planning
958 & Science Division. EMFAC data retrieved from: <https://www.arb.ca.gov/emfac/2014/>
- 959 California Energy Commission (2006) California Commercial End-Use Survey, CEC-400-2006-005. Retrieved
960 from: http://www.energy.ca.gov/ceus/2006_enduse.html (Aug 1, 2018).
- 961 Carranza, V., T. Rafiq, I. Frausto-Vicencio, F.M. Hopkins, K.R. Verhulst, P. Rao, R.M. Duren, C.E. Miller (2018)
962 Vista-LA: Mapping methane-emitting infrastructure in the Los Angeles megacity, *Earth Syst., Sci. Data*, **10**,
963 653-676, <https://doi.org/10.5194/essd-10-653-2018>.
- 964 Chavez, A., and A. Ramaswami, 2011: Progress toward low carbon cities: Approaches for transboundary GHG
965 emissions' footprinting. *Carbon Management*, **2**(4), 471-482, doi: 10.4155/cmt.11.38.

Christen, A., 2014: Atmospheric measurement techniques to quantify greenhouse gas emissions from cities. *Urban Climate*, **10**, 241-260, doi: 10.1016/j.uclim.2014.04.006.

Clark, S. S., and M. V. Chester, 2017: A hybrid approach for assessing the multi-scale impacts of urban resource use: Transportation in Phoenix, Arizona. *Journal of Industrial Ecology*, **21**(1), 136-150, doi: 10.1111/jiec.12422.

Commercial Building Energy Consumption Survey (2016) 2012 CBECS microdata files and information, U.S. Energy Information Administration. Data retrieved from: <https://www.eia.gov/consumption/commercial/data/2012/index.php?view=microdata> (Aug 1, 2018).

Davis, K.J., A. Deng, T. Lauvaux, N.L. Miles, S.J. Richardson, D. Sarmiento, K.R. Gurney, R.M. Hardesty, A. Brewer, P.B. Shepson, M.O. Cambaliza, C. Sweeney, J. Turnbull, J. Whetstone, A. Karion (2017) The Indianapolis Flux Experiment (INFLUX): A test-bed for developing anthropogenic greenhouse gas measurements, *Elem. Sci. Anth.*, **5**(21), <https://www.elementascience.org/article/10.1525/elementa.188/>

Department of Energy/Energy Information Administration 2003 Electric Power Monthly March 2003 Energy Information Administration, Office of Coal, Nuclear, and Alternate Fuels, US Department of Energy, Washington D.C. 20585. DOE/EIA form 923 reporting data retrieved from: <http://www.eia.gov/electricity/data/eia923> (July 27, 2018).

Department of Energy/Energy Information Administration (2018) State Energy Consumption Estimates 1960 through 2016, DOE/EIA-0214(2016), June 2018, Washington DC.

Djuricin, S., D. E. Pataki, and X. Xu, 2010: A comparison of tracer methods for quantifying CO₂ sources in an urban region. *J. of Geophys. Res.*, **115**(D11), doi: 10.1029/2009jd012236.

Federal Aviation Administration (2018a), OPSNET Manual: http://aspmhelp.faa.gov/index.php/OPSNET_Manual (Aug 1, 2018). Data retrieved from: <https://aspm.faa.gov/opsnet/sys/main.asp>.

Federal Aviation Administration (2018b), ETMSC Manual: http://aspmhelp.faa.gov/index.php/ETMSC_Manual (Aug 1, 2018). Data retrieved from: <https://aspm.faa.gov/tfms/sys/main.asp> (Aug 1, 2018).

Federal Emergency Management Agency (2017) HAZUS database. Retrieved from: <https://www.fema.gov/summary-databases-hazus-multi-hazard> (Aug 1, 2018).

Feng, S., Lauvaux, T., Newman, S., Rao, P., Ahmadov, R., Deng, A., Díaz-Isaac, L. I., Duren, R. M., Fischer, M. L., Gerbig, C., Gurney, K. R., Huang, J., Jeong, S., Li, Z., Miller, C. E., O'Keeffe, D., Patarasuk, R., Sander, S. P., Song, Y., Wong, K. W., and Yung, Y. L.: Los Angeles megacity: a high-resolution land-atmosphere modelling system for urban CO₂ emissions, *Atmos. Chem. Phys.*, **16**, 9019-9045, doi:10.5194/acp-16-9019-2016, 2016.

Fong, W. K., M. Sotos, M. Doust, S. Schultz, A. Marques, and C. Deng-Beck, 2014: *Global Protocol for Community-Scale Greenhouse Gas Emissions Inventories: An Accounting and Reporting Standard for Cities. WRI/C40/ICLEI*.

Font, A., Grimmond, C. S. B., Kotthaus, S., Morguí, J. A., Stockdale, C., O'Connor, E., ... Barratt, B. (2015). Daytime CO₂ urban surface fluxes from airborne measurements, eddy-covariance observations and emissions inventory in Greater London. *Environmental Pollution*. <https://doi.org/10.1016/j.envpol.2014.10.001>

1003 Getis, A., & Ord, J. K. (1992). The analysis of spatial association by use of distance statistics. *Geographical*
1004 *analysis*, 24(3), 189-206.

1005 Grimmond, C. S. B., T. S. King, F. D. Cropley, D. J. Nowak, and C. Souch, 2002: Local-scale fluxes of carbon
1006 dioxide in urban environments: Methodological challenges and results from Chicago. *Environmental Pollution*,
1007 116(SUPPL. 1). [https://doi.org/10.1016/S0269-7491\(01\)00256-1](https://doi.org/10.1016/S0269-7491(01)00256-1)

1008 Gurney, K.R., D. Mendoza, Y. Zhou, M Fischer, S. de la Rue du Can, S. Geethakumar, C. Miller (2009) [The Vulcan](#)
1009 [Project: High resolution fossil fuel combustion CO₂ emissions fluxes for the United States](#), *Environ. Sci.*
1010 *Technol.*, 43(14), 5535-5541, doi:10.1021/es900806c.

1011 Gurney K.R., Huang J and Coltin K 2014 Comment on quick, J C (2014) carbon dioxide emission tallies for 210 US
1012 coal-fired power plants: a comparison of two accounting methods *J. Air Waste Manage. Assoc.* 64: 73–79, *J.*
1013 *Air Waste Manage. Assoc.*, 64 1215–7

1014 Gurney, K.R., J. Huang and K. Coltin (2016) [Bias present in US federal agency power plant CO₂ emissions data and](#)
1015 [implications for the US clean power plan](#), *Env. Res. Lett.*, 11, 064005, doi: 10.1088/1748-9326/11/6/064005.

1016 Gurney, K.R., J. Liang, R. Patarasuk, D. O’Keeffe, J. Huang, M. Hutchins, T. Lauvaux, J. C. Turnbull, and P. B.
1017 Shepson, 2017: Reconciling the differences between a bottom-up and inverse-estimated FFCO₂ emissions
1018 estimate in a large U.S. urban area. *Elementa: Science of the Anthropocene*, 5, 44, doi: 10.1525/elementa.137.

1019 Gurney, K.R., Liang, J, D.O. O’Keeffe, R. Patarasuk, M. Hutchins, J. Huang, P. Rao, and Y. Song (2018)
1020 Comparison of Global Downscaled Versus Bottom-Up Fossil Fuel CO₂ Emissions at the Urban Scale in Four
1021 US Urban Areas, *J. Geophys. Res.-Atmos.*, <https://doi.org/10.1029/2018JD028859>.

1022 Gurney K.R., J. Liang, D. O’Keeffe, J. Huang, Y. Song, P. Rao, T.M. Wong (2019), Hestia Fossil Fuel Carbon
1023 Dioxide (FFCO₂) Data Product - Los Angeles Basin, Version 2.5, 1km grid,
1024 <https://doi.org/10.18434/T4/1502503> (last accessed December 20, 2018).

1025 Heimberger Heimburger, AMF, Shepson, PB, Stirn, BH, Susdorf, C, Turnbull, J, et al. 2017 Precision Assessment
1026 for the Aircraft Mass Balance Method for Measurement of Urban Greenhouse Gas Emission Rates. *Elem Sci*
1027 *Anth*: In press for the INFLUX Special Feature

1028 Hirsch, J. & Associates (2004) *Energy Simulation Training for Design & Construction Professionals*. Retrieved
1029 from: <http://doe2.com/download/equest/eQuestTrainingWorkbook.pdf> (Aug 1, 2018). eQuest model download
1030 available from: <http://www.doe2.com/eQuest/> (Aug 1, 2018).

1031 Homer, C.G., Dewitz, J.A., Yang, L., Jin, S., Danielson, P., Xian, G., Coulston, J., Herold, N.D., Wickham, J.D.,
1032 and Megown, K., 2015: [Completion of the 2011 National Land Cover Database for the conterminous United](#)
1033 [States-Representing a decade of land cover change information](#). *Photogrammetric Engineering and Remote*
1034 *Sensing*, v. 81, no. 5, p. 345-354

1035 Hopkins, F. M., Kort, E. A., Bush, S. E., Ehleringer, J., Lai, C., Blake, D., and Randerson, J. T. 2016: Spatial
1036 patterns and source attribution of urban methane in the Los Angeles Megacity, *J. Geophys. Res.-Atmos.*, 121,
1037 2490–2507, <https://doi.org/10.1002/2015JD024429>

1038 Hutyra, L. R., R. Duren, K. R. Gurney, N. Grimm, E. A. Kort, E. Larson, and G. Shrestha, 2014: Urbanization and
 1039 the carbon cycle: Current capabilities and research outlook from the natural sciences perspective. *Earth's*
 1040 *Future*, **2**(10), 473-495, doi: 10.1002/2014ef000255.
 1041 Intergovernmental Panel on Climate Change "IPCC guidelines for national greenhouse gas inventories, Prepared by
 1042 the National Greenhouse Gas Inventories Programme" (IGES, Japan, 2006).
 1043 Jones, C., and D. M. Kammen, 2014: Spatial distribution of U.S. household carbon footprints reveals
 1044 suburbanization undermines greenhouse gas benefits of urban population density. *Environmental Science and*
 1045 *Technology*, **48**(2), 895-902, doi: 10.1021/es4034364.
 1046 Kort, E. A., C. Frankenberg, C. E. Miller, and T. Oda, 2012: Space-based observations of megacity carbon dioxide.
 1047 *Geophys. Res. Lett.*, **39**(17), doi: 10.1029/2012gl052738.
 1048 Lauvaux, T., Miles, N.L., Richardson, S.J., Deng, A., Stauffer, D., et al. 2013: Urban emissions of CO₂ from Davos,
 1049 Switzerland: the first real-time monitoring system using an atmospheric inversion technique. *J. Appl Meteor.*
 1050 *and Climatol.*, **52**: 2654–2668. doi: <https://doi.org/10.1175/JAMC-D-13-038.1>
 1051 Lauvaux, T., Miles, N. L., Deng, A., Richardson, S. J., Cambaliza, M. O., Davis, K. J., Gaudet, B., Gurney, K. R.,
 1052 Huang, J., O'Keefe, D., Song, Y., Karion, A., Oda, T., Patarasuk, R., Razlivanov, I., Sarmiento, D., Shepson, P.,
 1053 Sweeney, C., Turnbull, J. and Wu, K.: High-resolution atmospheric inversion of urban CO₂ emissions during
 1054 the dormant season of the Indianapolis Flux Experiment (INFLUX), *J. Geophys. Res. Atmos.*, **121**(10), 5213–
 1055 5236, doi:10.1002/2015JD024473, 2016.
 1056 Le Quéré, C., Andrew, R. M., Friedlingstein, P., Sitch, S., Pongratz, J., Manning, A. C., Korsbakken, J. I., Peters, G.
 1057 P., Canadell, J. G., Jackson, R. B., Boden, T. A., Tans, P. P., Andrews, O. D., Arora, V. K., Bakker, D. C. E.,
 1058 Barbero, L., Becker, M., Betts, R. A., Bopp, L., Chevallier, F., Chini, L. P., Ciais, P., Cosca, C. E., Cross, J.,
 1059 Currie, K., Gasser, T., Harris, I., Hauck, J., Haverd, V., Houghton, R. A., Hunt, C. W., Hurtt, G., Ilyina, T., Jain,
 1060 A. K., Kato, E., Kautz, M., Keeling, R. F., Klein Goldewijk, K., Körtzinger, A., Landschützer, P., Lefèvre, N.,
 1061 Lenton, A., Lienert, S., Lima, I., Lombardozi, D., Metzl, N., Millero, F., Monteiro, P. M. S., Munro, D. R.,
 1062 Nabel, J. E. M. S., Nakaoka, S.-I., Nojiri, Y., Padin, X. A., Peregon, A., Pfeil, B., Pierrot, D., Poulter, B.,
 1063 Rehder, G., Reimer, J., Rödenbeck, C., Schwinger, J., Séférian, R., Skjelvan, I., Stocker, B. D., Tian, H.,
 1064 Tilbrook, B., Tubiello, F. N., van der Laan-Luijkx, I. T., van der Werf, G. R., van Heuven, S., Viovy, N.,
 1065 Vuichard, N., Walker, A. P., Watson, A. J., Wiltshire, A. J., Zaehle, S., and Zhu, D.: Global Carbon Budget
 1066 2017, *Earth Syst. Sci. Data*, **10**, 405-448, <https://doi.org/10.5194/essd-10-405-2018>, 2018.
 1067 Lin, J.C., Mitchell, M., Buchert, E., Crosman, E., Mendoza, D., Gurney, K.R., Patasuruk, R., Bowling, D., Pataki,
 1068 D., Bares, R., Fasoli, B., Catherine, D., Baasandorj, M., Jacques, A., Hoch, S., Horel, J., and Ehleringer, J.
 1069 (2018) CO₂ and carbon emissions from cities: linkages to air quality, socioeconomic activity and stakeholders in
 1070 the Salt Lake City urban area, *Bull Am. Meteorological Soc.*, **99**(11), 2325–2339. [https://doi.org/10.1175/bams-](https://doi.org/10.1175/bams-d-17-0037.1)
 1071 [d-17-0037.1](https://doi.org/10.1175/bams-d-17-0037.1)
 1072 Los Angeles County (2016) Countywide Building Outlines – 2014 Update – Public Domain Release. Retrieved
 1073 from: [https://egis3.lacounty.gov/dataportal/2016/11/03/countywide-building-outlines-2014-update-public-](https://egis3.lacounty.gov/dataportal/2016/11/03/countywide-building-outlines-2014-update-public-domain-release/)
 1074 [domain-release/](https://egis3.lacounty.gov/dataportal/2016/11/03/countywide-building-outlines-2014-update-public-domain-release/) (Aug 1, 2018).

1075 Los Angeles World Airports (2014), Personal communication: Norene Hastings, Environmental Supervisor, Los
 1076 Angeles World Airports, Environmental Services division, January 2014.
 1077 Manufacturing Energy Consumption Survey (2010) 2010 MECS Survey Data, U.S. Energy Information
 1078 Administration. Retrieved from: <https://www.eia.gov/consumption/manufacturing/data/2010/#r10> (Aug 1,
 1079 2018).
 1080 Marion, W. and Urban, K. 1995. *User's Manual for TMY2s Typical Meteorological Years*. National Renewable
 1081 Energy Laboratory (NREL), <http://rredc.nrel.gov/solar/pubs/tmy2/PDFs/tmy2man.pdf>, accessed date July 22,
 1082 2014.
 1083 Martin, C.R., N Zeng, A. Karion, K. Mueller, S. Ghosh, I. Lopez-Coto, K.R. Gurney, T. Oda, K. Prasad, Y. Liu,
 1084 R.R. Dickerson, J. Whetstone (2018): Investigating Sources of Variability and Error in Simulations of Carbon
 1085 Dioxide in an Urban Region, *Atmos. Env.*, 199, 55-69. <https://doi.org/10.1016/j.atmosenv.2018.11.013>
 1086 Mays, KL, Shepson, PB, Stirm, BH, Karion, A, Sweeney, C, et al. 2009: Aircraft-Based Measurements of the
 1087 Carbon Footprint of Indianapolis. *Environmental Science & Technology*, **43**(20): 7816–7823. DOI:
 1088 <https://doi.org/10.1021/es901326b>
 1089 McKain, K., A. Down, S. M. Raciti, J. Budney, L. R. Hutyrá, C. Floerchinger, S. C. Herndon, T. Nehrkorn, M. S.
 1090 Zahniser, R. B. Jackson, N. Phillips, and S. C. Wofsy, 2015: Methane emissions from natural gas infrastructure
 1091 and use in the urban region of Boston, Massachusetts. *Proceedings of the National Academy of Sciences USA*,
 1092 **112**(7), 1941-1946, doi: 10.1073/pnas.1416261112.
 1093 Menzer, O., W. Meiring, P. C. Kyriakidis, and J. P. McFadden, 2015: Annual sums of carbon dioxide exchange over
 1094 a heterogeneous urban landscape through machine learning based gap-filling. *Atmospheric Environment*, **101**,
 1095 312-327, doi: 10.1016/j.atmosenv.2014.11.006.
 1096 Miles, NL, Richardson, SJ, Lauvaux, T, Davis, KJ, Deng, A, et al. 2017: Quantification of urban atmospheric
 1097 boundary layer greenhouse gas dry mole fraction enhancements: Results from the Indianapolis Flux Experiment
 1098 (INFLUX), *Elem. Sci. Anth.*, **5**(0), 27. <https://doi.org/10.1525/elementa.127>.
 1099 Mitchell, L., J.C. Lin, D.R. Bowling, D.E. Pataki, C. Strong, A.J. Schauer, R. Bares, S.E. Bush, B.B. Stephens, D.
 1100 Mendoza, D. Mallia, L. Holland, K.R. Gurney, J.R. Ehleringer (2018) Long-term urban carbon dioxide
 1101 observations reveal spatial and temporal dynamics related to urban characteristics and growth, *Proceedings of*
 1102 *the National Academy of Sciences*. March 5, 2018, <https://doi.org/10.1073/pnas.1702393115>
 1103 Mount, D.M. and S. Arya (2010) ANN: A Library for Approximate Nearest Neighbor Searching, Version 1.1.2,
 1104 Release Date: Jan 27, 2010. Retrieved from: <https://www.cs.umd.edu/~mount/ANN/> (Aug 1, 2018).
 1105 Newman, S., Xu, X., Gurney, K. R., Hsu, Y. K., Li, K. F., Jiang, X., Keeling, R., Feng, S., O’Keefe, D., Patarasuk,
 1106 R., Wong, K. W., Rao, P., Fischer, M. L., and Yung, Y. L.: Toward consistency between trends in bottom-up_
 1107 CO₂ emissions and top-down atmospheric measurements in the Los Angeles megacity, *Atmos. Chem. Phys.*, **16**,
 1108 3843–3863, <https://doi.org/10.5194/acp-16-3843-2016>, 2016.
 1109 Patarasuk, R., Gurney, K. R., O’Keefe, D., Song, Y., Huang, J., Rao, P., Buchert, M., Lin, J. C., Mendoza, D., and
 1110 Ehleringer, J. R.: Urban high-resolution fossil fuel CO₂ emissions quantification and exploration of emission

1111 drivers for potential policy applications, *Urban Ecosyst.*, 19, 1013–1039, [https://doi.org/10.1007/s11252-016-](https://doi.org/10.1007/s11252-016-0553-1)
1112 0553-1, 2016.

1113 Porse, E., J. Derenski, H. Gustafson, Z. Elizabeth, and S. Pincetl, 2016: Structural, geographic, and social factors in
1114 urban building energy use: Analysis of aggregated account-level consumption data in a megacity. *Energy*
1115 *Policy*, **96**, 179–192, doi: 10.1016/j.enpol.2016.06.002.

1116 Portland Cement Company, Economic Research Department (2006) *U.S. and Canadian Portland Cement Industry*
1117 *Plant Information Summary*, Portland Cement Association, Skokie, IL.

1118 Quick J 2014 Carbon dioxide emission tallies for 210 US coal- fired power plants: a comparison of two accounting
1119 methods *J. Air Waste Manage. Assoc.* 64 73–9

1120 Performance Measurement System (PeMS) Data Source: <http://www.dot.ca.gov/trafficops/mpr/source.html> (Aug 1,
1121 2018).

1122 Ramaswami, A., T. Hillman, B. Janson, M. Reiner, and G. Thomas, 2008: A demand-centered, hybrid life-cycle
1123 methodology for city-scale greenhouse gas inventories. *Environmental Science and Technology*, **42**(17), 6455–
1124 6461, doi: 10.1021/es702992q.

1125 Rao, P., Gurney, K. R., Patarasuk, R., Yang, S., Miller, C. E., Duren, R. M., and Eldering, A. **2017**: Spatio-temporal
1126 variations in on-road CO₂ emissions in the Los Angeles Megacity, *ALMS Geosci.*, 3, 239–267,
1127 <https://doi.org/10.3934/geosci.2017.2.239>.

1128 Residential Energy Consumption Survey (2013) 2009 RECS Survey Data, U.S. Energy Information Administration.
1129 Retrieved from: <https://www.eia.gov/consumption/residential/data/2009/index.php?view=microdata> (Aug 1,
1130 2018).

1131 Richardson, S. J., Miles, N. L., Davis, K. J., Lauvaux, T., Martins, D. K., Turnbull, J. C., ... Cambaliza, M. O. L.
1132 (2017). Tower measurement network of in-situ CO₂, CH₄, and CO in support of the Indianapolis FLUX
1133 (INFLUX) Experiment. *Elem Sci Anth*, 5(0), 59. <https://doi.org/10.1525/elementa.140>

1134 Sargent, M., Barrera, Y., Nehrkorn, T., Hutyrá, L. R., Gately, C. K., Mckain, K., ... Jones, T. (2018). Correction for
1135 Sargent et al., Anthropogenic and biogenic CO₂ fluxes in the Boston urban region. *Proceedings of the*
1136 *National Academy of Sciences*, 115(40), E9507–E9507. <https://doi.org/10.1073/pnas.1815348115>

1137 Schwandner, F. M., Gunson, M. R., Miller, C. E., Carn, S. A., Eldering, A., Krings, T., ... Podolske, J. R. (2017).
1138 Spaceborne detection of localized carbon dioxide sources. *Science*, 358(6360).
1139 <https://doi.org/10.1126/science.aam5782>

1140 Seto, KC, Dhakal, S, Bigio, A, Blanco, H, Delgado, GC, et al. 2014 Human Settlements, Infrastructure and Spatial
1141 Planning. In: *Climate Change 2014: Mitigation of Climate Change*. Contribution of Working Group III to the
1142 Fifth Assessment Report of the Intergovernmental Panel on Climate Change [Edenhofer, O, Pichs-Madruga, R,
1143 Sokona, Y, Farahani, E, Kadner, S, Seyboth, K, Adler, A, Baum, I, Brunner, S, Eickemeier, P, Kriemann, B,
1144 Savolainen, J, Schlömer, S, von Stechow, C, Zwickel, T and Minx, JC (eds.)]. Cambridge University Press,
1145 Cambridge, United Kingdom and New York, NY, US.

1146 Shu, Y., and N. S. N. Lam, 2011: Spatial disaggregation of carbon dioxide emissions from road traffic based on
 1147 multiple linear regression model. *Atmospheric Environment*, **45**(3), 634-640, doi:
 1148 10.1016/j.atmosenv.2010.10.037.
 1149 Southern California Association of Governments (2012) Parcel Data GIS Shapefiles. Retrieved by personal
 1150 communication from Kimberly S. Clark (Clark@scag.ca.gov) and Christine Fernandez
 1151 (fernandez@scag.ca.gov).
 1152 Southern California Association of Governments (2014) SCAG AWDT data, personal communication, Mike
 1153 Ainsworth (AINSWORT@scag.ca.gov), Transportation Modeling, Air Quality & Conformity, October, 2014.
 1154 Staufer, J., Broquet, G., Bréon, F. M., Puygrenier, V., Chevallier, F., Xueref-Rémy, I., ... Ciais, P. (2016). The first
 1155 1-year-long estimate of the Paris region fossil fuel CO₂ emissions based on atmospheric inversion. *Atmospheric
 1156 Chemistry and Physics*, **16**(22), 14703–14726. <https://doi.org/10.5194/acp-16-14703-2016>
 1157 Turnbull, J. C., Sweeney, C., Karion, A., Newberger, T., Lehman, S. J., Tans, P. P., Davis, K. J., Lauvaux, T., Miles,
 1158 N. L., Richardson, S. J., Cambaliza, M. O., Shepson, P. B., Gurney, K., Patarasuk, R. and Razlivanov, I.:
 1159 Toward quantification and source sector identification of fossil fuel CO₂ emissions from an urban area: Results
 1160 from the INFLUX experiment, *J. Geophys. Res. Atmos.*, **120**(1), 292–312, doi:10.1002/2014JD022555, 2015.
 1161 United States Environmental Protection Agency (1995) FIRE Version 5.0 Source Classification Codes and Emission
 1162 Factor Listing for Criteria Air Pollutants, EPA-454/R-95-012. Retrieved from
 1163 <https://www3.epa.gov/ttn/chief/old/efdocs/454r95012.pdf> (July 27, 2018).
 1164 United States Environmental Protection Agency (2013) Facility Registry Service (FRS). Setting Up A Data Flow
 1165 with FRS: FRS Information Needs. Retrieved from [https://www.epa.gov/frs/setting-data-flow-frs-
 1166 information-needs](https://www.epa.gov/frs/setting-data-flow-frs-information-needs) (Aug 1, 2018).
 1167 United States Environmental Protection Agency (2015a) Technical Support Document (TSD) Preparation of
 1168 Emissions Inventories for the Version 6.2, 2011 Emissions Modeling Platform. Retrieved from
 1169 <https://www.epa.gov/air-emissions-modeling/2011-version-62-technical-support-document> (July 27, 2018).
 1170 United States Environmental Protection Agency (2015b) 2011 National Emissions Inventory, version 2 Technical
 1171 Support Document. Document retrieved from [https://www.epa.gov/air-emissions-inventories/2011-national-
 1172 emissions-inventory-nei-technical-support-document](https://www.epa.gov/air-emissions-inventories/2011-national-emissions-inventory-nei-technical-support-document) (July 27, 2018). NEI version 2.0 data retrieved from:
 1173 <https://www.epa.gov/air-emissions-inventories/2011-national-emissions-inventory-nei-data> (July 27, 2018).
 1174 United States Environmental Protection Agency (2015c), 40 DFR Part 60, EPA-HQ-OAR-2013-0602; FRL-XXXX-
 1175 XX-OAR, RIN 2060-AR33, Carbon Pollution Emission Guidelines for Existing Stationary Sources: Electric
 1176 Utility Generating Units, August 3, 2015. Air Markets Program Data 2012 Pre-packaged data retrieved from:
 1177 <ftp://ftp.epa.gov/dmdnload/emissions/hourly/monthly/> (May 28, 2012).
 1178 USGS (2003) *Minerals Yearbook, Vol. 1, Metals and Minerals, 2002*. U.S. Geological Survey. U.S. Department of
 1179 the Interior. July 2003
 1180 VandeWeghe, J. R., and C. Kennedy, 2007: A spatial analysis of residential greenhouse gas emissions in the
 1181 Toronto census metropolitan area. *Journal of Industrial Ecology*, **11**(2), 133-144, doi: 10.1162/jie.2007.1220.

1182 Velasco, E., and M. Roth, 2010: Cities as net sources of CO₂: Review of atmospheric CO₂ exchange in urban
 1183 environments measured by eddy covariance technique. *Geography Compass*, **4**(9), 1238-1259, doi:
 1184 10.1111/j.1749-8198.2010.00384.x.
 1185 Velasco, E., S. Pressley, E. Allwine, H. Westberg, and B. Lamb, 2005: Measurements of CO₂ fluxes from the
 1186 Mexico City urban landscape. *Atmospheric Environment*, **39**(38), 7433-7446, doi:
 1187 10.1016/j.atmosenv.2005.08.038.
 1188 Verhulst, K. R., Karion, A., Kim, J., Salameh, P. K., Keeling, R. F., Newman, S., Miller, J., Sloop, C., Pongetti, T.,
 1189 Rao, P., Wong, C., Hopkins, F. M., Yadav, V., Weiss, R. F., Duren, R. M., and Miller, C. E.: Carbon dioxide
 1190 and methane measurements from the Los Angeles Megacity Carbon Project – Part 1: calibration, urban
 1191 enhancements, and uncertainty estimates, *Atmos. Chem. Phys.*, **17**, 8313–8341, [https://doi.org/10.5194/acp-17-](https://doi.org/10.5194/acp-17-8313-2017)
 1192 8313-2017, 2017
 1193 Whetstone, J.R. (2018) Advances in urban greenhouse gas flux quantification: The Indianapolis Flux Experiment
 1194 (INFLUX). *Elem. Sci. Anth.*, **6**: 24. doi: <https://doi.org/10.1525/elementa.282>
 1195 Wong, C. K., Pongetti, T. J., Oda, T., Rao, P., Gurney, K. R., Newman, S., Duren, R. M., Miller, C. E., Yung, Y. L.,
 1196 and Sander, S. P.: Monthly trends of methane emissions in Los Angeles from 2011 to 2015 inferred by CLARS-
 1197 FTS observations, *Atmos. Chem. Phys.*, **16**, 13121–13130, [https://doi.org/10.5194/acp-16-](https://doi.org/10.5194/acp-16-13121-2016) 13121-2016, 2016.
 1198 Wong, K. W., Fu, D., Pongetti, T. J., Newman, S., Kort, E. A., Duren, R., Hsu, Y.-K., Miller, C. E., Yung, Y. L.,
 1199 and Sander, S. P.: Mapping CH₄:CO₂ ratios in Los Angeles with CLARS- FTS from Mount Wilson, California,
 1200 *Atmos. Chem. Phys.*, **15**, 241–252, <https://doi.org/10.5194/acp-15-241-2015>, 2015
 1201 WRI/WBCSD, 2004: *The Greenhouse Gas Protocol: A Corporate Accounting and Reporting Standard*. World
 1202 Business Council for Sustainable Development and the World Resources Institute.
 1203 [<http://www.ghgprotocol.org/corporate-standard>]
 1204 Wu, K, Lauvaux, T, Davis, KJ, Deng, A, Lopez Coto, I, Gurney, KR and Patarasuk, R 2018: Joint inverse estimation
 1205 of fossil fuel and biogenic CO₂ fluxes in an urban environment: An observing system simulation experiment to
 1206 assess the impact of multiple uncertainties. *Elem. Sci. Anth.* doi: <http://doi.org/10.1525/elementa.138>
 1207 Wunch, D., Wennberg, P. O., Toon, G. C., Keppel-Aleks, G., and Yavin, Y. G.: Emissions of greenhouse gases from
 1208 a North American megacity, *Geophys. Res. Lett.*, **36**, 1–5, <https://doi.org/10.1029/2009GL039825>, 2009.
 1209 Zhou, Y. Y., and K. R. Gurney, 2011: Spatial relationships of sector-specific fossil fuel CO₂ emissions in the United
 1210 States. *Global Biogeochemical Cycles*, **25**, GB3002, doi: 10.1029/2010gb003822.